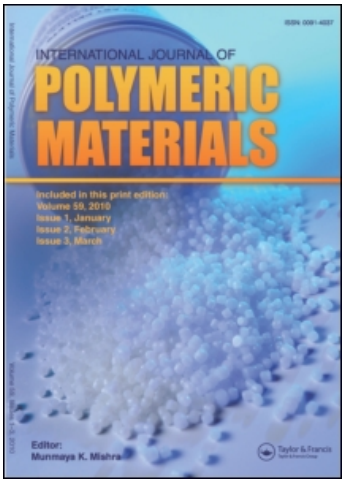

International Journal of Polymeric Materials
Publication details, including instructions for authors and subscription information:
http://www.informaworld.com/smpp/title~content=t713647664

Ultra High Strength, High Modulus Polyethylene Spectra Fibers and Composites

S. Kavesh[a]; D. C. Prevorsek[a]
[a] AlliedSignal Inc., Morristown, N.J., USA

To cite this Article Kavesh, S. and Prevorsek, D. C.(1995) 'Ultra High Strength, High Modulus Polyethylene Spectra Fibers and Composites', International Journal of Polymeric Materials, 30: 1, 15 — 56
To link to this Article: DOI: 10.1080/00914039508031459
URL: http://dx.doi.org/10.1080/00914039508031459

Intern. J. Polymeric Mater., 1995, Vol. 30, pp. 15–56
Reprints available directly from the publisher
Photocopying permitted by license only

Ultra High Strength, High Modulus Polyethylene Spectra Fibers and Composites

S. KAVESH and D. C. PREVORSEK
AlliedSignal Inc., Morristown, N.J. USA

(Received September 26, 1994)

SPECTRA® polyethylene fibers are rapidly gaining acceptance in many applications in which high strength and modulus are required. They also represent a breakthrough in fiber technology because they represent the first case of a successful conversion of a flexible polymer into an ultra-strong fiber. Until the work of Pennings, who did the pioneering work on solution processing of ultra high molecular weight polyethylene, it was postulated that the manufacture of very strong extended chain fibers requires special rigid polymers that form nematic liquid crystalline solutions or melts. The driving force for the commercial success of Spectra® is based not only on its specific modulus and strength but also on its unmatched damage tolerance and impact resistance. In this study, we identify the molecular, crystallographic and morphological factors contributing to the fatigue and impact resistance and damage tolerance of this fiber.

KEY WORDS Polyethylene, fibers, strength, modulus, morphology, crystal defects, damage tolerance.

INTRODUCTION

SPECTRA® polyethylene fibers have the highest strength of any man-made fiber and a unique and exceptional combination of strength, modulus and toughness. They are beneficially applied in artificial tendons, ligaments and joint prosthesis. Protective gloves with remarkable cut resistance are saving the hands of surgeons and numerous workers. Sport equipment such as kayaks, canoes, bicycles, boats, sails, skis and others are employing SPECTRA® fibers to provide toughness and strength at low weight. SPECTRA® fibers and SPECTRA SHIELD® are protecting lives of our police and our military in bullet resistant vests, helmets and armor.

PROCESS DEVELOPMENT

To place Spectra® into perspective something must be said about its background and genesis.

Polymer molecules are long chain compounds with simple repeating units generally containing carbon-carbon bonds. Science has long recognized that because of the intrinsic strength of the carbon-carbon bond, a polymeric material could theoretically possess extraordinary properties if composed of perfectly crystallized, fully extended molecules. Unfortunately, all known processes for preparing fibers gave rise to "folded chain" molecular structures which inefficiently distributed the load and were therefore weak. The challenge was to devise a practical process which could prepare fibers in which the molecules were in the extended state.

One approach to this problem was to synthesize special polymers with "rigid rod" segments which did not have as great a tendency to fold. Such polymers are expensive to synthesize, difficult to spin into fibers and require strong, corrosive and toxic chemicals to process. The approach taken by the authors was to devise simple, safe methods for chain extending common and inexpensive, flexible macromolecules. SPECTRA® polyethylene was the first material mastered and commercialized.

Polyethylene had been an article of commerce for almost fifty years. It had also been one of the most extensively studied of all materials. Chemical abstracts lists 67,786 references to polyethylene in the period 1967–1986. Historically, polyethylene has been known as a low strength, low stiffness material—the squeeze bottle plastic. However, theory indicated that because of the small cross-section of the polyethylene chain, fully extended polyethylene would have a high packing density and because of the strength of the carbon-carbon bond, could be extraordinarily strong.

Indeed, in the years 1979–1983, several processes were proposed by others who succeeded in preparing laboratory specimens of extended chain fibers. Most notably, the authors recognize their debt to the pioneering work of Albertus Pennings and his associates at the University of Groeningen, The Netherlands. However, none of these products or processes were successful outside of the laboratory environment.

The high performance polyethylene (PE) fibers available to date are made by a solution spinning process that evolved from the Couette flow surface growth experiments of Pennings.[1] By studying the mechanisms of fiber formation in the Couette flow experiments, Pennings and his students, Smith, Lemstra and Kalb[2] developed the principles for solution spinning of ultra-high molecular weight polyethylene as well as a process disclosed in the patent which represents the foundation of DSM technology for producing Dyneema fibers.[3]

Parallel research at AlliedSignal resulted in a solution spinning process developed by Kavesh and Prevorsek.[4] These fibers are available commercially under the trade name of Spectra® 900 and 1000. In addition to the process development research that is covered by several U.S. patents, Prevorsek and his collaborators at AlliedSignal Corporate Technology Center and the team of J.J. Dunbar at AlliedSignal Fibers in Petersburg, dedicated a great deal of research to applications and Spectra® fiber composites. The combined efforts of these two groups resulted in a portfolio of more than 100 U.S. patents and pending patent applications. These include Spectra-Shield® and a variety of composites used in soft and rigid armor. It was this research that led to the discovery of i) large strain-rate effects, that are unique for polyeth-

ylene fibers, and contribute to the unmatched impact resistance of these fibers, ii) the role of the nano-scale microstructure which resembles that of the sea shells and contributes to the damage tolerance of Spectra® fibers and composites, and iii) the role of solid state transformations in PE crystals that contribute to the energy absorption potential, resistance to repeated impact, and abrasion and fatigue resistance of these fibers.

The first simple practical route to preparation of extended chain fibers which could be practiced economically on a commercial scale was described in AlliedSignal patent U.S.P. #4,414,110, November 1, 1983. The approach taken consisted of preparing a solution of the polymer, spinning the solution into fiber with several novel steps taken to prevent the formation of structures (spherulites) which could interfere with later chain extension and then stretching and chain extending the fiber at a temperature above its normal melting point. The materials used in processing are safe to operating personnel and to end-users.

Equally important, as a consequence of the success of this approach, U.S.P. #4,413,110 described novel polyethylene fibers of extremely high specific modulus (three-fourth that of diamond), greater specific strength and toughness than any previous man-made fiber, and higher melting point than other gel-spun polyethylene fibers. The AlliedSignal fibers were commercialized under the trade name SPECTRA® in 1985 within the short space of two years through the combined efforts of many AlliedSignal contributors and the vision of its management.

ORIGINS OF DAMAGE TOLERANCE, PENETRATION AND FATIGUE RESISTANCE

Spectra® fibers exhibit outstanding mechanical properties. For comparison with other reinforcing fibers we show in Figure 1 their specific modulus and strength. However, the commercial success of Spectra® fibers cannot be explained solely on the basis of these properties. Their commercial success must also be attributed to their unmatched damage tolerance and fatigue resistance.[5] The ability of these fibers to fail in shear and/or compression without losing a great deal of tensile strength is a unique characteristic of polyethylene and represents a distinct advantage over other reinforcing materials. This is particularly important when the products are used in the technology of survival, where the primary function of a part is to protect primary structures, people or equipment from the blasts of explosions and impact of fast moving projectiles, etc. In this section we will identify the properties or combination of properties that make SPECTRA fibers particularly suitable for the applications that represent the foundation for their successful commercialization. Focusing, therefore, on their unique damage tolerance, fatigue and abrasion resistance, and the capability of delayed recovery after an apparently plastic deformation, we will identify the molecular and morphological origins of these properties and review the fundamental differences between PE and other high performance fibers.

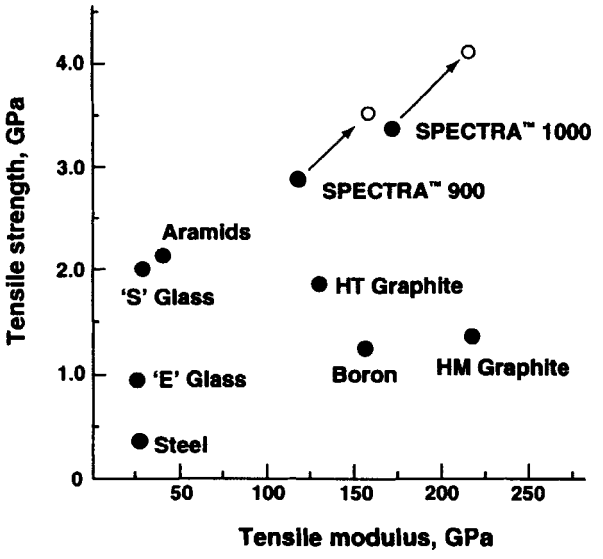

FIGURE 1 Specific tensile strength vs. specific modulus showing Spectra 900 and Spectra 1000 fiber with other fibers. Arrows and open circles indicate the improvements in properties with increasing rate of deformation. This strain-rate effect is unique with PE fibers.

MORPHOLOGY OF ULTRA-STRONG PE FIBERS

Ultra-strong polyethylene fibers produced by solution spinning exhibit morphology that is typical for all organic fibrous materials. Spectra as well as other polyethylene fibers exhibit a well defined aggregate structure on a macro (50 nm) as well as microfibrillar level (5 nm). Fundamental differences that may exist between PE and other high performance organic fibers, such as polyaramids, rigid rod and thermotropic LC fibers, must therefore originate in the longitudinal characteristics of these fibers and especially in the microfibril and interfibrillar matter. A generalized structural model representing the key characteristics of fibrous materials is shown in Figure 2. Small angle X-ray diffraction studies of Grubb,[6] electron microscopy of the authors[7] and especially the studies of Schaper *et al.*[8] provide a great deal of information relative to dimensional characteristics of the microfibrils.

It has been established by these techniques that high strength high modulus PE consists of microfibrils whose lateral dimension is well defined and amounts to ~4 nm. The studies of Schaper[8] indicate that the microfibrils have a finite length of about 1000 to 2000 nm. This yields a microfibril aspect ratio L/D of 250–500. In addition, the small angle x-ray diffraction work of Grubb[6] indicates the presence of a long period of ~200 nm. This means that the structure of the microfibril is not uniform in density, but contains areas of different density that could be attributed to domains containing a high concentration of crystal defects. These findings are supported by the electron microscopy work of Kramer[7] at Allied-Signal. Based on the analysis of mechanical properties and degrees of crystallinity measured by WAXS, we propose that these disordered domains whose longitudinal dimensions appear to be 4–5 nm are "amorphous" domains that may contain a substantial

MORPHOLOGY OF MAN-MADE FIBERS

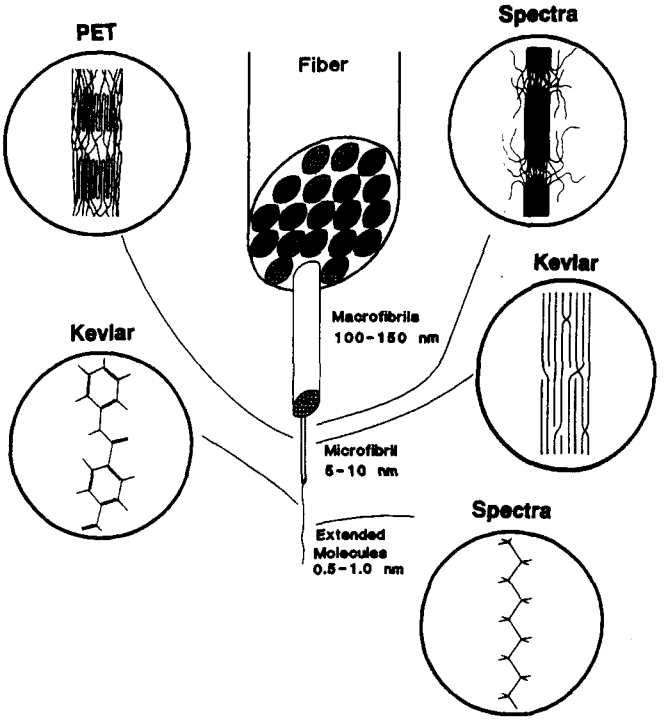

FIGURE 2 Hierachical morphology of organic polymeric fibers.

TABLE I

Characteristics of the microfibril of the ultra-strong PE fibers

Microfibril diameter	:	~4nm
Microfibril L/D	:	250-500
Nearly perfect crystal L/D	:	~40
Amorphous domain linking covalently needle like crystals L/D	:	1

amount of chain ends. It is important to note that this "amorphous" domain is covalently bonded to the adjacent nearly perfect, needle-like crystalline domains whose L/D is 40. The characteristics of the microfibril of the ultra-strong PE Fibers are summarized in Table I.

The needle-like nearly perfect crystalline domains exhibit a crystal size in (002) direction that is detected by WAXS but does not give rise to small angle X-ray diffraction. Since the periodicity does not involve density fluctuation, we attribute

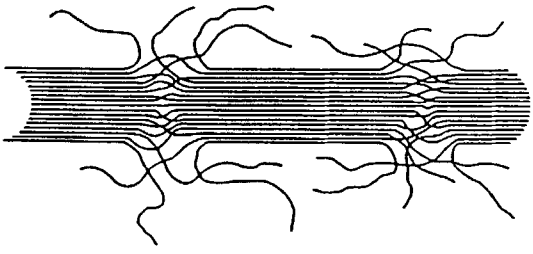

FIGURE 3 Model of microfibril of ultra-high molecular weight Spectra polyethylene fiber (from Reference 9).

the crystallite size in the 002 direction to the twist boundaries that are discussed in the next section. A schematic model of the microfibril is shown in Figure 3.

DEFECTS IN CRYSTALLINE POLYETHYLENE

Based on the structural model shown in Figure 3, a molecule of high molecular weight polyethylene containing 10^5 or more CH_2 groups in the chain is likely to contain several molecules that traverse crystalline domains that are 10–20 nm long and contain 100–200 CH_2 units in their crystallographic direction. Considering the very short crystallization and deformation times, it is obvious that these crystals must contain a large amount of crystal defects. While these defects play an important role in the deformation and mechanical properties of all flexible organic polymers, their role is much more important in polyethylene than in any other polymers. This is due to the very small CH_2 repeating unit, the flexibility of the C—C bond and low rotational barriers as well as low forces between the chains. This allows the incorporation of various defects into the crystal lattice with much smaller increments in energy of the crystal than any other organic polymers.

Reneker[9] identified and characterized several defects in a single polyethylene molecule which can form a crystallographic defect in a polyethylene crystal. Computer modeling showed that these defects can diffuse along the molecue and, through this process, translate and/or rotate the molecule, transport free volume or bring together reaction sites. The existence of such defects has been proven in single crystals of polyethylene. It has also been shown that the interactions of a specific conformational defect of a single molecule (dispiration) with the strain field in a lamellar crystal lead to mechanical relaxation which occurs in the region of time and temperature corresponding to the alpha relaxation process.

Since the background on the defects is essential to explain the drawing behavior of PE fibers, its creep and damage tolerance, we present below an overview of the defects that play a role in these phenomena. The schematic model of Figure 4 represents the planar zig-zag backbone of the molecule by a flat ribbon which can twist around its longitudinal axis or bend round a traverse axis. The net amount of twist in each defect is indicated by the crossing of the edges in the ribbon. The

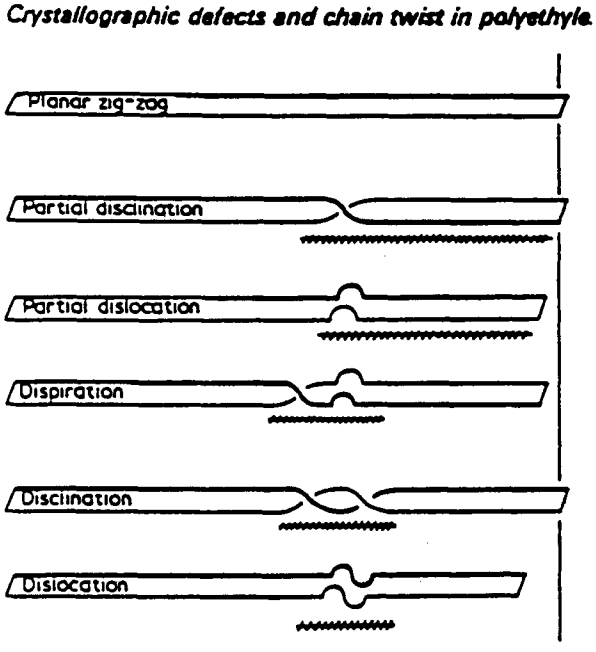

FIGURE 4 Schematic illustration of crystallographic defects in a polyethylene molecule (from Reference 9).

bent segments indicate the presence of one extra CH_2 group in the dispiration and partial dislocation or two extra CH_2 groups in the dislocation. The presence of extra CH_2 groups shortens the ribbon by a corresponding amount indicated at the right end. The regions where the packing energy of the molecules significantly exceeds the packing energy of a planar zig-zag molecule in a perfect crystal are indicated by a cross hatched line. Note that the partial defects force the part of the molecule on one side of the defect to a higher energy position that extends indefinitely while the complete defects have a finite extent. The ribbon model is used in the later figures to portray actual minimum energy conformations of various defect structures.

Since the chain folding in lamellar crystals requires chain bending as well as chain twisting, the twist in the crystal can be, upon drawing, transferred into the "unfolded crystals." Reneker *et al.*[9] addressed this problem as follows. A segment of a polyethylene crystal folded in a (110) plane is shown in Figure 5. Note a ribbon emerging from the top of the crystal must bend 180° and then twist so that the ribbon plane is correctly oriented to reenter the crystal. The amount of twist required depends upon the sense of the twist, being either twice the setting angle or twice the difference between 90° and the setting angle. The setting angle for polyethylene crystals is approximately 48° with respect to the *b* axis. When the twisted ribbon reaches the bottom surface of the lamellar crystal the ribbon must first twist (or untwist) by approximately 90° so that a bend will return the chain to a proper lattice position. Figure 6a shows a ribbon in which the sense of the twist is the same at the top and bottom so that each fold adds approximately 90° of net twist to the ribbon. Figure 6b shows the alternative in which the twist at the top

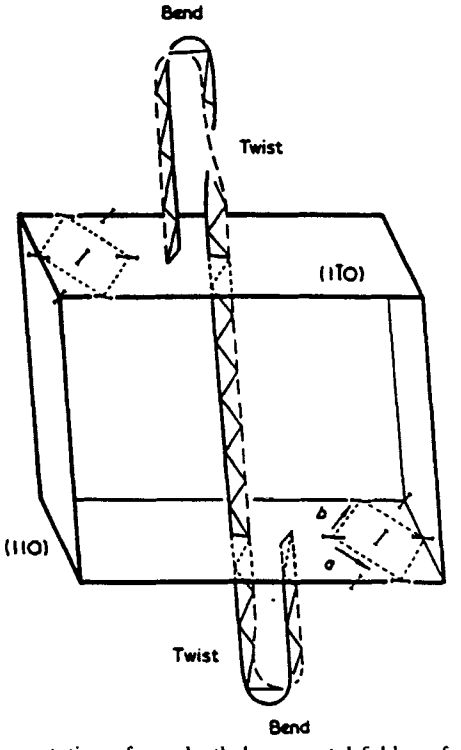

FIGURE 5 Schematic representation of a polyethylene crystal fold conformation in a (110) plane (from Reference 9).

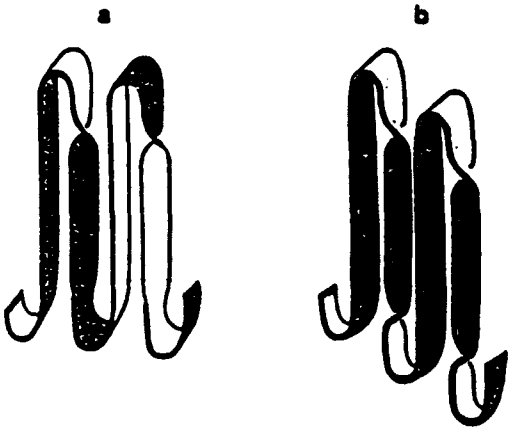

FIGURE 6 Schematic representation of folded ribbon twist conformations a) Twist at the top, b) Twist at the top and untwist at the bottom (from Reference 9).

fold cancels the twist at the bottom, leaving zero twist. Because the energy differences between the two possibilities appear to be small, the general case may involve some canceling but leave the ribbon with a reasonable amount of twist.

A folded chain ribbon with (110) folds and 90° non-canceling twist are incor-

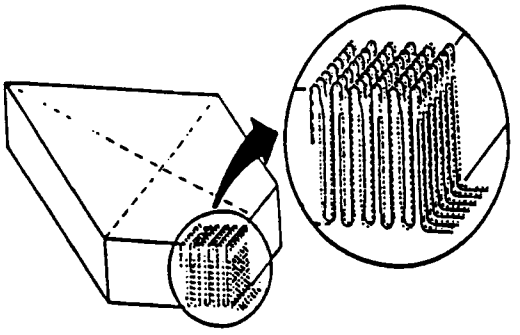

FIGURE 7 A lamellar crystal of polyethylene with (110) fold plane (from Reference 9).

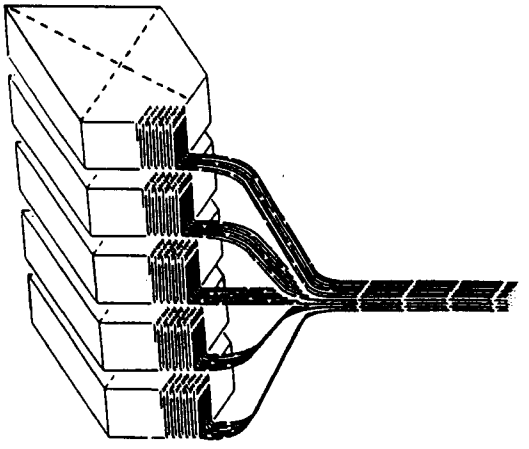

FIGURE 8 Schematic illustration of the conversion of lamellar crystals into a fiber (from Reference 9).

porated into a lamellar crystal in Figure 7. Reneker[9] also proposed a mechanical deformation process that draws the folded ribbons into a fiber. Since electron micrographs indicate that adjacent lamellae generally cooperate in such a process, fibers from any adjacent lamellae are incorporated into a polyethylene fiber. The drawing process creates a necked region in which short, randomly spaced segments are not in the planar zig-zag conformation. A simplified diagram of the neck is shown in Figure 8. As the molecules pack together in the fiber the twist aggregates into boundaries. The twist boundaries interact with other defects to establish low density boundaries by transporting free volume to the boundary.

TWIST BOUNDARIES IN FIBERS

Severe packing problems occur as twisted polyethylene molecules pack together in a fiber during cold drawing. The cost in terms of packing energy of accommodating the twist can be minimized if the twist in all the adjacent chains is segregated into a transverse plane not necessarily perpendicular to the chain axis. This arrangement does not affect the excess energy of the twist significantly, but it does

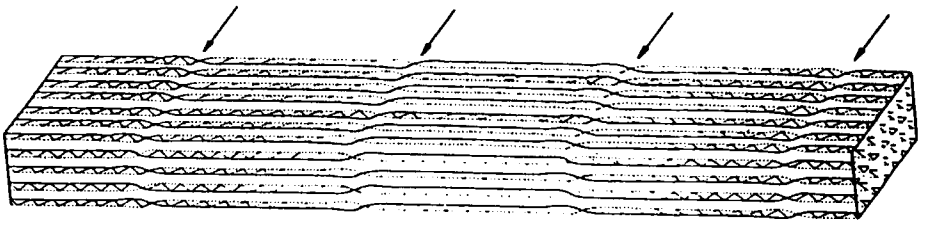

FIGURE 9 Enlarged portion of Figure 8 (from Reference 9).

TABLE II

Energies associated with chain defects in a 60 atom—polyethylene crystal

Defect	Length (Atoms)	Energy Kcal mol^{-1}
Dispersion	6	11.8
Disclination	4	17.2
Dislocation	8	23.6

minimize the lengths of the chain segments that are not at the lowest packing energy value of the setting angle. In its perfect form, a twist boundary can be regarded as a type of twin boundary, that is, a boundary that establishes a specific and recurrent non-crystallographic geometric relationship between two crystal lattices. Twist boundaries with either 180° or 90° of twist in each chain as it passes through the boundary are both possible in polyethylene. Figure 9 which is an enlargement of part of Figure 8, shows a small fiber containing four 180° twist boundaries. The separation between these boundaries is determined by the amount of twist that is present in the polyethylene molecules as they emerge from the drawing process and are incoporated in the crystalline fiber. A repulsive force between boundaries that is transmitted elastically through the intervening planar zig-zag segments would tend to produce periodic separation of the boundaries. If the twist boundaries contain only 90° of twist, either for dynamic reasons or because of lower energy, then twice as many boundaries are required to accommodate a given amount of twist.

Reneker[9] proposed that the twist boundary separation is an important parameter in establishing the long period in a fiber. Chain ends, vacancies, folds and other defects may be trapped at the twist boundaries or subsequently migrate there. Since the perfect twist boundary has nearly the same density as the crystal, it does not lead to the small angle X-ray or electron scattering. Hence, a perfect twist boundary should give rise to a crystallite size by wide angle X-ray diffraction but would not be detectable by small angle X-ray diffraction. The (002) crystallite size obtained by WAXS could, therefore, correspond to the twist boundary.

The 100–200 nm scale periodicity observed by Grubb[6] by small angle X-ray diffraction and indicated by electron microscopy is, on the other hand, associated with domains of lower density. Reneker[9] proposed that these low density domains

represent the accumulation of free volume at twist boundaries resulting from the transport of chain ends and folds. In the absence of "morphological" data about the structure of this "low density" element, we regard, on the basis of mechanical analyses, these highly disordered domains as tight amorphous domains containing a great number of chain ends, loops and folds. The strength of this domain is considerably lower than that of the needle-like crystal and so is its molecular weight. Since the strength of fiber is controlled by the strength of its weakest element, the strength of these fibers is considerably below the strength predicted by a flawless ensemble of polymer molecules. The extra energies associated with these defects have been calculated by Reneker[9] and are given in Table II.

All these energies are below the breaking energy of a C—C bond (~80 Kcal/mol) and can be activated by both heat and mechanical stress. It should also be noted that, because of the size of CH_2 group and low inter-chain forces, the energies of these defects are much lower than those of corresponding defects in PVA. Considering that an important factor affecting the solid state stretchability of a fiber forming polymer is the ratio of energies to form and transport chain defects through a crystal to energy to break the polymer backbone, it follows that solid state PVA will be much less stretchable than PE. This has indeed been observed.

So far, we discussed the role and characteristics of small single chain defects. It has been recognized that larger defects can also exist. Keith and Passaglia[10] described edge screw dislocations which can move inside the lamella crystals and Predecki and Statton[11] suggested that screw dislocations provide a way to accommodate chain ends inside a polymer crystal as shown in Figure 10. Note that a chain fold can be accommodated in the same way.

If we envision the crystallization process of a high molecular weight and highly extended PE proceeding from two adjacent nuclei, the domain between the crystals does contain not only a high concentration of chain defects and free volume transported to the crystal boundaries but also many cross-over points of polymer domains. These cross-overs develop when a molecule transverse two adjacent crystals has a different position in one crystal than the other. Because these cross-overs

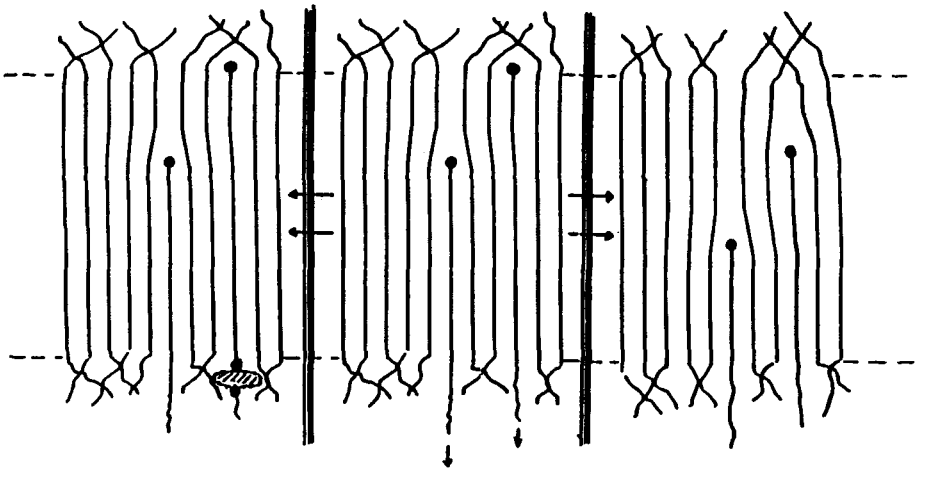

FIGURE 10 Dislocation rearrangement of chain ends in polyethylene.

add to the strain of the amorphous molecules, they provide an additional mechanism to stop the growth of the adjacent crystals in the microfibril. It can be assumed that in two crystals that contain a large fraction of same molecules, the disordered domain between the crystals must contain many cross-over points. However, such cross-overs can also exist in the crystals to form crystallographic defects called twist disclinations. Since their motion along the chains can be activated by heat and stress, we propose that formation and motions of such defects play an important role in mechanical properties of all semicrystalline polymers and especially polyethylene.

Because of the small repeating unit and low intermolecular interactions in the crystals of PE relative to other polymers used in man made fibers, it is very clear that the solid state rearrangements discussed above occur at much lower stress and temperature than those with any other polymeric fiber commercially available.

It is especially important to note that these solid state nanometer deformations are not only very important in the formation of fibers and creep behavior but also represent a major energy absorption mechanism when PE fibers are used in composites designed to absorb energy. This latter aspect of solid state deformations is discussed below.

STRESS DISTRIBUTION

To analyze the mechanical properties and especially the modulus in terms of the morphological characteristics discussed above, it is necessary to determine or assume a stress distribution. A great deal of work relative to this problem has been done using Takayanagi models.[12] However, considering the uncertainties associated with the choice of an adequate model, it is desirable to consider more realistic approaches based on experimental data from strained fibers.

The most fundamental issue raised by some authors is whether the stress is homogeneously or inhomogeneously distributed throughout the sample. In case of homogeneous stress distributions, the stress applied to the sample equals the stress experienced by the crystalline regions. The existence of a homogeneous stress distribution in PE was first proposed by Sakurada.[13] He determined the modulus of crystalline domains of various PE samples assuming that the stress applied to each sample correlated with the crystalline modulus according to $E_1 = \sigma/\varepsilon_c$ where σ is the applied stress and ε_c is the lattice extension. However, the determinations of E_1 for a set of samples with different microstructures yielded in all cases $E_1 =$ 235 GPa despite large variations in specimen modulus Y_1 (0.65–15.0 GPa). Therefore, Sakurada inferred that in strained PE samples, the stress distribution is homogeneous (see Table III). Ward,[14,15] on the other hand, reported much lower E_1 of 150 GPa. He proposed that part of the crystalline regions are in parallel with amorphous regions as a "crystalline bridge" and reproduced the modulus using a series-parallel type of Takayanagi model.

In an attempt to resolve this issue of stress distribution, Nakamae *et al.*[16] recently completed a very comprehensive study relative to the sample and crystalline modulus in PE. These authors investigated the ten samples listed in Table IV. For each

TABLE III

Elastic moduli of different specimens of polyethylene

Specimen	Density g/cm^{-3}	Crystallinity (%)	E_1 (GPa)	Y_1 (GPa)	E_1/Y_1
High-tenacity fiber	0.971	84	235	15	16
Film	0.962	78	235	7.0	34
Film, γ-irradiated and drawn	0.961	77	235	4.8	50
Film	0.945	67	225	3.1	74
Monofilament	0.941	64	235	2.4	100
Low-density film, drawn and γ-irradiated	0.924	52	235	0.65	370

sample, they determined: specimen modulus, crystallite sizes by WAXS, long period by SAXS, lattice constant, density, degree of crystallinity, melting point, heat of fusion and degree of orientation. While the various morphological characteristics of these samples vary a great deal and especially that the specimen modulus varied for 0.4 to 207.5 GPa, the crystalline modulus of all samples determined by the shift in (002) reflection was constant at 235 GPa. This seemingly confirmed once more that the stress in polyethylene crystals is homogeneous.

Experimental evidence supporting the heterogeneous stress distribution is provided by Micro-Raman spectroscopy. Kip et al.[17] used experimental solution spun ultra-high molecular weight polyethylene fibers with different draw ratio. They do not disclose the spinning and drawing conditions but the final draw ratio characteristics are listed in Table V. Raman spectra were obtained at 295 ± ,0.5°K using a Jobin-Yvon Ramanor HG2S double monocrometer. The 514 mm line of Ar laser was used for actuation.

Raman spectra from strained fibers were obtained using a deformation device attached onto the microscope stage. The recorded spectra has a resolution of 5 cm^{-1} and the investigated range was between 950 and 1160 cm^{-1}. Both the asymmetric and symmetric C—C stretching modes fall into this region. The results of this study provided evidence of the existence of two types of strained molecules.

To reach this conclusion, the authors[17]:

- Fitted both the asymmetric and symmetric C—C stretching bands with two Gaussian curves (Figure 11)

TABLE IV

Characteristics of PE different microstructures

Characteristic	1	2	3	4	5	6	7	8	9	10
Specimen modulus (GPa)	56.3	22.4	63.3	83.3	105.9	207.5	100.2	0.4	4.65	---
Crystallite size (Å)										
(002)	386	325	520	630	468	927	711	106	161	653
(200)	105	210	92	137	119	172	158	71	79	456
(020)	117	162	101	142	119	178	151	112	110	285
Long period (Å)	285	369	*a*	*a*	*a*	*a*	*a*	183	218	*a*
Lattice constant										
a (Å)	7.46	7.41	7.39	7.39	7.43	7.43	7.41	7.59	7.50	7.41
b (Å)	4.94	4.94	4.94	4.93	4.95	4.94	4.94	4.99	4.95	4.93
Density (g/cm^3)	0.969	0.977	0.976	0.976	0.974	0.991	0.984	0.919	0.924	0.994
Crystallinity (%)	81.1	86.1	85.5	85.5	84.3	94.5	90.2	48.0	51.5	96.4
Melting point (°C)	143	142	146	147	143	148	148	123	120	141
Heat of fusion (cal/g)	60.9	61.8	61.7	57.7	58.9	60.1	56.8	22.5	32.8	---
Degree of orientation	0.976	0.973	0.988	0.990	0.985	0.994	0.982	0.940	0.981	0.969

a Not observed

TABLE V

Specifications of UHMW-PE fibers

Fiber	Cross-sectional area (10^{-10} m^2)	Strength[a] (GPa)	Young's modulus[b] (GPa)
A1	2.8	1.3	28
A2	1.9	2.2	62
A3	1.0	3.0	100
A4	1.1	3.1	121
B1	1.5	3.4	114
B2	0.67	4.9	172
B3	0.57	5.1	202

[a]Strain rate 0.083 s^{-1}

[b]Strain rate 0.083 s^{-1}, initial modulus

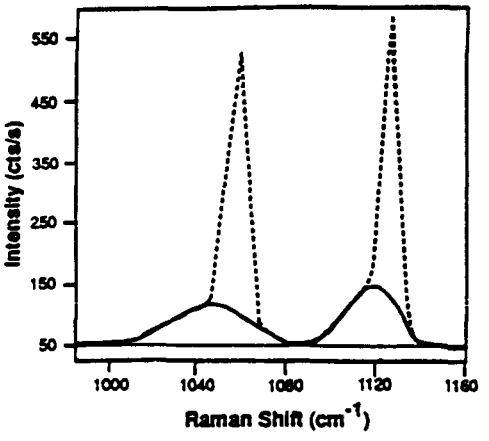

FIGURE 11 Raman spectrum of PE fiber A3 (in Table V) at 2.5% strain (from Reference 17).

- Established the frequency shift/stress ratio of the broad (small) and narrow (large) component (Figures 12 and 13)
- Determined that the strain ratio of the two components is in the order of one magnitude
- Estimated that the fraction of C—C bonds exhibiting high strain is ~40%

The authors established that:

- The shift at a given applied strain is directly proportional to the fiber modulus (Figure 14)

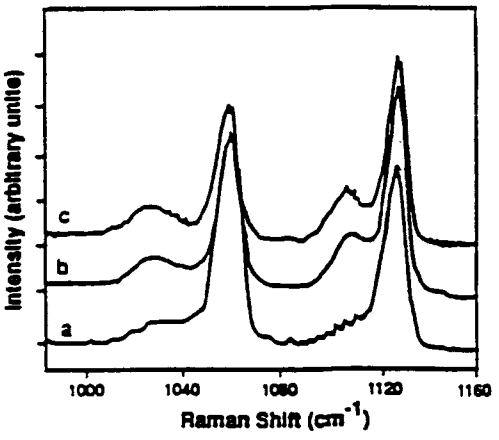

FIGURE 12 Raman spectra after applying 3.0% strain: a: A3 fiber, b: B2 fiber and c: B3 fiber (in Table V).

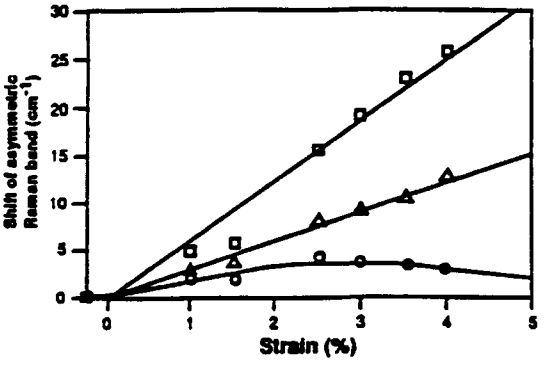

FIGURE 13 Positions of asymmetric C—C stretching bands as a function of strain for the A3 fiber in Table V. (Broad, mean and narrow band form the top) (from Reference 17).

- The width of the broad band (FWHM) increases with increasing strain but the increase for the asymmetric stretching mode is about 30% higher than that of symmetric stretching mode.

Since the publication of this work, the laser-Raman studies similar to those of Kip *et al.*[17] were carried out by Grubb[34] as well as Young.[18] Since their data agree with the finding of Kip *et al.*, it is very clear that there is a wide distribution of stresses in polyethylene samples and that continuation of this work would provide complementary information relative to the structure of these fibers.

Kip *et al.*[17] were also investigating whether this technique could be used to explain the "drawability" of a fiber. To answer this question they examined two fibers produced by different processing conditions and stretched to achieve the equal modulus of ~100 GPa. They found that the fiber with higher width of the broad band exhibited lower residual drawability than the fiber with a narrow strain distribution. Thus, an important and useful correlation has been observed between drawability and strain distribution.

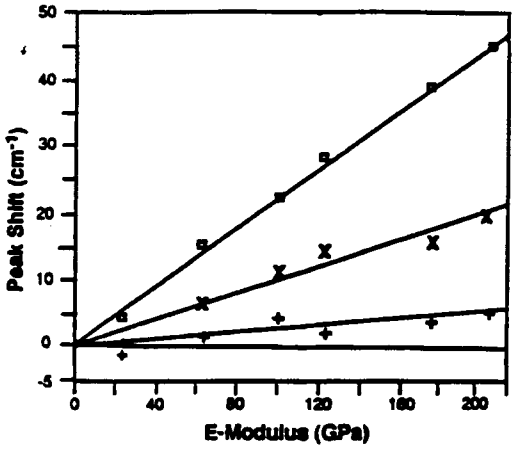

FIGURE 14 Shift of asymmetric C—C stretching modes at 4.0% strain as a function of Young's modulus. (Broad, mean and narrow band from the top).

The first clues regarding the obvious discrepancies between the homogeneous stress hypothesis advanced by Sakurada[13] and Nakamae[16] and the wide stress distribution indicated by the work of Kip *et al.*[17] come from the stress-relation experiments followed by Raman spectroscopy. This work was done simultaneously in several laboratories yielding similar results.

Here we report the work of Young.[18] Using Spectra 1000 fibers, Young subjected single filament to various levels of constant strain (2%, 4%, 6%, 8%, 10% and 15%) over periods of time up to 6000 sec. The corresponding shifts for the narrow and broad peak are shown in Figures 15–18. The dotted lines represent the peak positions in the unstrained samples. These data show that, in a stress relaxation experiment, the position of the peak approaches that of the unstrained samples and, in some cases, some of the C—C bonds appear to be compressed in comparison with their state in unstretched samples. The differences between the positions of the two peaks decreases almost by a factor of four within 10 sec.

These results clearly show the complexity and time dependence of stress distribution. Realizing that time dependent stress distribution may be the cause of an apparently homogeneous stress as advocated by Sakurada *et al.*[13] and Nakemae *et al.*,[16] Kip *et al.*[19] carried out WAXS analyses from strained Dyneema (149 GPa modulus) fibers. They found that the equational and meridional diffractograms as function of the strain recorded at 240°K showed no changes in "a" and "b" unit cell dimensions, no indications of crystallite breaking and no indication for transformation of the orthorhombic into monoclinic or hexagonal phase. In *c*-direction of the orthorhombic phase, a bi-modal strain distribution is observed indicating that part of the crystals are strained significantly more than the rest (Figure 19). The WAXS analyses carried out at Allied-Signal Inc.[20] using Spectra 1000 fiber produced essentially the same results.

Based on this additional work of Kip *et al.*,[19] it can be concluded that at least, in ultra-high modulus polyethylene fibers, we have a distribution of stresses in the orthorhombic crystalline phase. It is also clear that in the samples under constant strain, the distribution of stress changes with times, because the strain of the highly

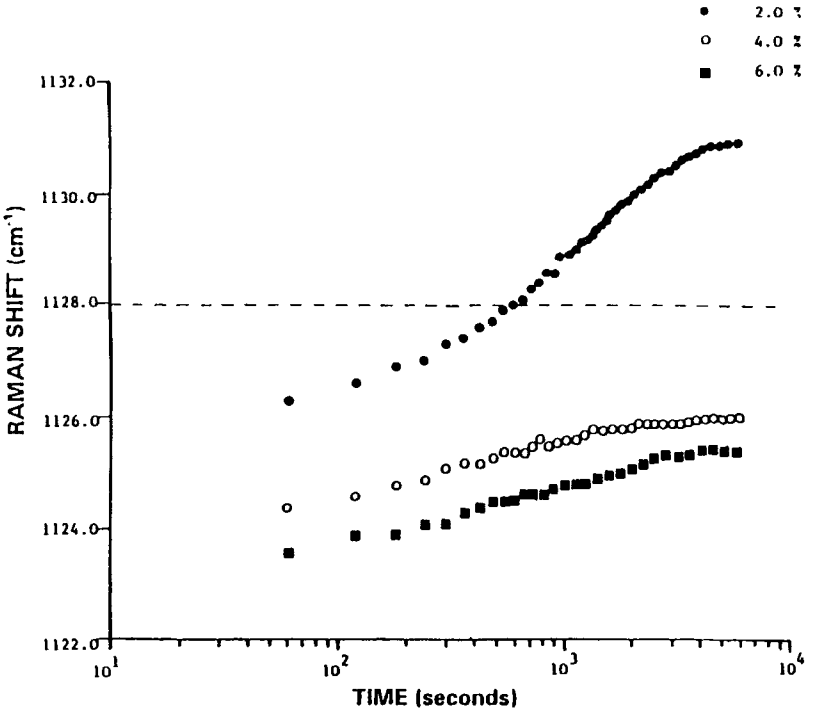

FIGURE 15 Raman shift of narrow peak for Spectra 1000 at 2.0, 4.0 and 6.0% strain.

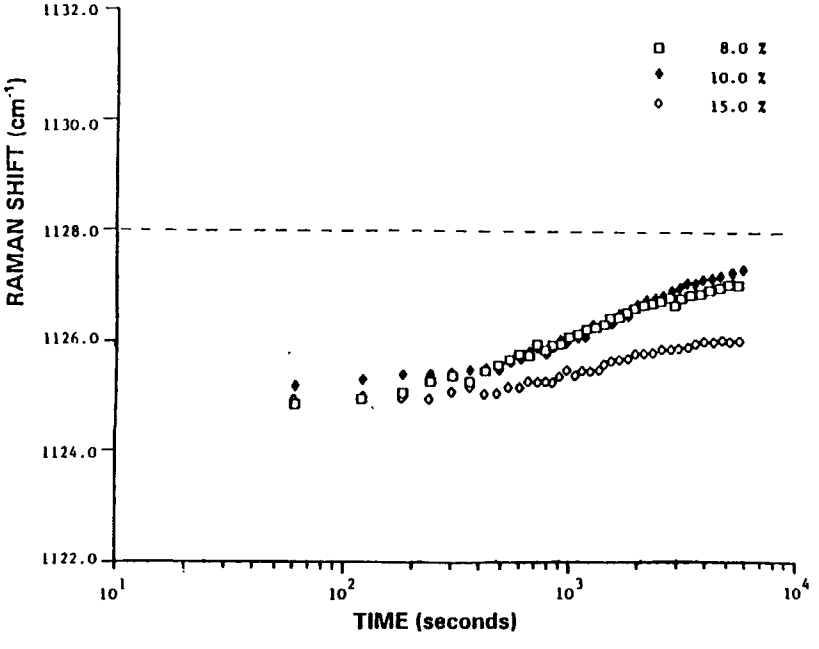

FIGURE 16 Raman shift of narrow peak for Spectra 1000 at 8.0, 10.0 and 15.0% strain.

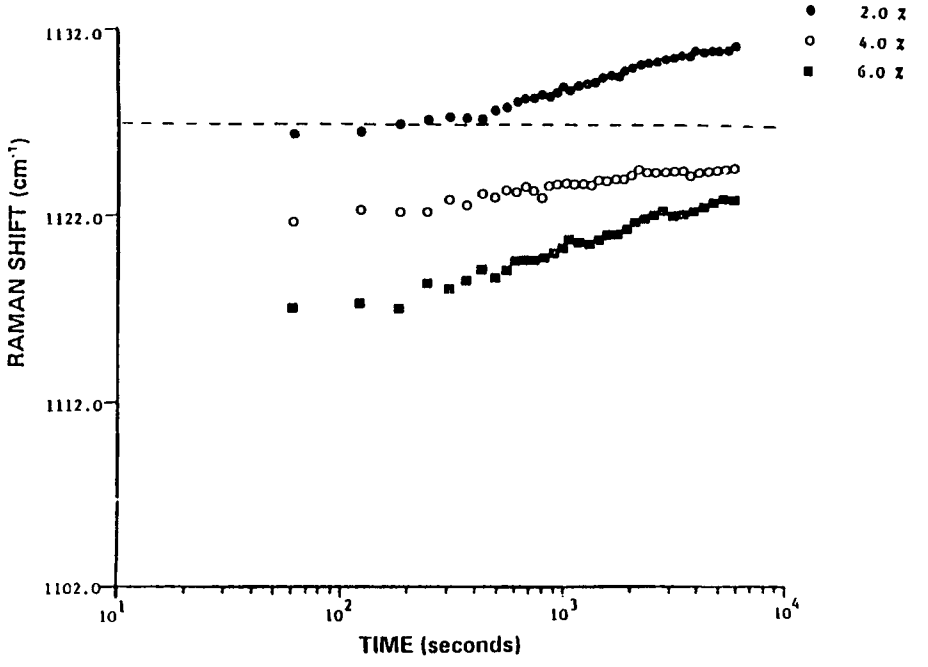

FIGURE 17 Raman shift of broad peak for Spectra 1000 at 2.0, 4.0 and 6.0% strain.

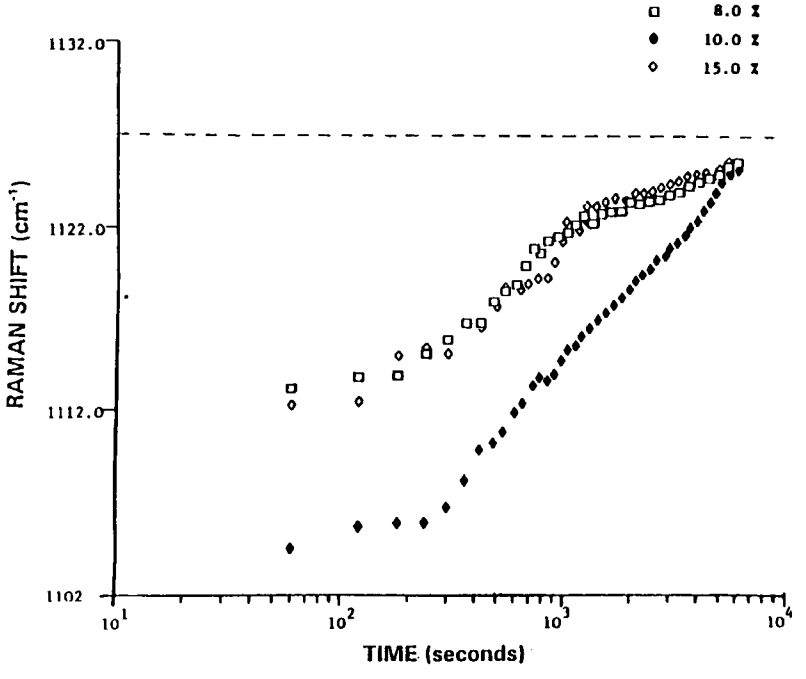

FIGURE 18 Raman shift of broad peak for Spectra 1000 at 8.0, 10.0 and 15.0% strain.

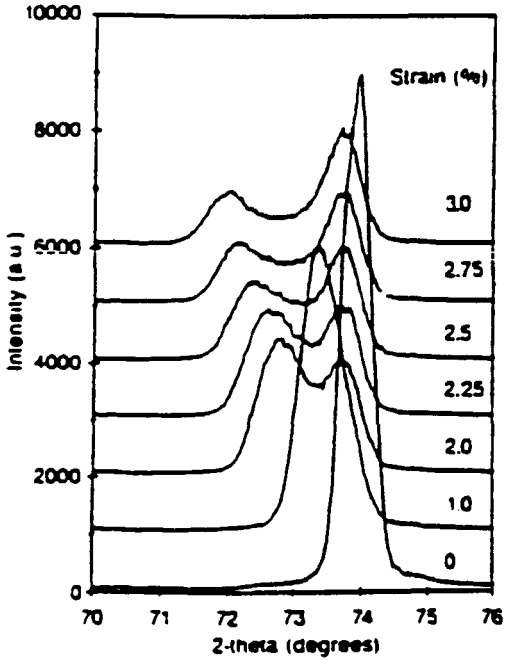

FIGURE 19 Meridional diffractograms of polyethylene fiber at different levels of strain (from Reference 19).

strained phase is decaying faster than that of the low strain component. A micromechanical analysis of Prevorsek *et al.* has shown the stress distribution in PE crystals in Spectra® fibers is the consequence of crystals' large length/diameter ratio.[35]

Modulus

Crystalline modulus has been the subject of numerous experimental and theoretical studies. Nakamae *et al.*[16] reported recently a comprehensive summary of reported values for the crystalline modulus in the direction parallel to the chain axis. From the data in Table VI, it is clear that both theoretical and experimental results vary a great deal. Most of the experimental data fall in the range between 230 and 340 GPa while the calculated values are generally higher and fall mostly in the 280–420 GPa range with a few exceptions on the lower side (Treloar[21] 182 GPa in 1960) and on the high side (Deward *et al.*[22] 494 GPa in 1979).

Considering that the distribution of stress is non-homogeneous and that the disordered regions amount to ~25% of the volume fraction of the fiber, the value of 235 GPa reported by Sakurada and Nakamae must be considered as the lower bound and the actual value must be significantly higher. Considering further that the low temperature measurements of the Nakamae yielded, at −155°C, a crystalline modulus of 254 GPa, it can be further inferred that the actual modulus of the crystalline domains is higher than 254 GPa at 155°C. Therefore, the value of

TABLE VI

Observed and calculated E_1 values of polyethylene already reported

Methods	E_1 (GPa)	Authors	Year
X-ray diffraction	235 (r.t)	Sakurada et. al	1962
	235 (r.t)	Sakurada et. al	1964
	196 (r.t)	Miyasaka et. al	1966
	255 (-165°C)	Ward et. al.	1978
	150 (r.t.)	Ward et. al.	1978
	266 (r.t)	Ward et. al.	1979
	213-229 (r.t)	Matuso et. al.	1986
	235 (r.t)	In this study	
	254 (-155°C)	In this study	
Raman scattering	340	Mizushima et. al.	1949
	358	Schauffele et. al.	1967
	290	Strobl et. al.	1976
	281	Kobayashi et. al.	1983
Neutron scattering	329	Feldkamp et. al.	1968
	329	Twisleton et. al.	1972
nfrared spectrum	267	Wool et. al.	1986
Calculated	182	Treloar	1960
	340	Shimanouchi et. al.	1962
	290	Miyazawa	1965
	256	Odajima et. al.	1966
	160	Alfrey	1966
	316	Kitgawa	1968
	285	Frank	1970
	324	Wobser	1970
	243	Shiro et. al.	1971
	297	Boudreaux	1973
	221-245	Perepelkin et. al.	1974
	380	McCullough et. al.	1977
	316	Tashiro et. al.	1978
	494	Dewar et. al.	1979
	405	Crist et. al.	1979
	420	Brower et. al.	1980
	345-406	Karpfen	1981
	305	Suhai	1983
	351	Sorenson et. al.	1988
Observed	262 (288, -196°C)	Barham et. al.	1979
	220 (r.t)		
	216 (r.t)	Kanamoto et. al.	1983
	232 (r.t)	Matsuo et. al.	1988
		Kunugi et. al.	1988

$E_1 \approx 300 \pm 20$ GPa seems the most realistic range consistent both with experimental and theoretical analyses. This is also consistent with the theoretical value of 290 GPa proposed by Boudreaux.[23]

Based on the structural model presented above, in which roughly 25% of the fiber volume is in the rubbery state, and existence of nanometer defects that can transport the chain through the crystals under the effect of stress and temperature

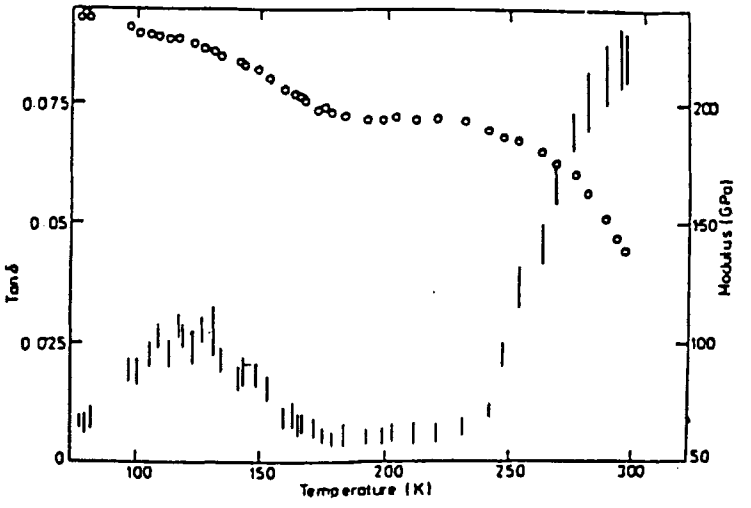

FIGURE 20 Tensile modulus of polyethylene fiber and loss factor (Tan δ) as a function of temperature.

is anticipated that modulus of ultra-strong PE fibers is strain rate dependent, this is indeed the case.

We investigated the modulus of Spectra fiber by a variety of techniques and equipment including transverse impact using high velocity projectiles. By combining all the measurements, we obtain an almost five-fold increase in modulus as the strain rate increases by about five orders of magnitude from 10^2 to 10^4 min^{-1}. At ballistic rates of deformations, based on these data, the room temperature modulus approaches 300 GPa.

It should also be noted that transverse impact data analyzed by the method of Smith[24] also yield a value of fiber modulus ~300 GPa, which agrees well with our data obtained using high speed testing equipment. Transverse impact on fibers using direct measurements of strain wave propagation yields, for the same fiber, significantly lower values of modulus between 160–200 GPa depending on the rate of deformation and pretension. This shows the difficulties in selecting proper modulus data in the analysis of the behavior of structures made of ultra-strong polyethylene fibers.

The effect of temperature on modulus of ultra-high modulus fibers was investigated by Barham and Keller.[25] Their results are shown in Figure 20. Their estimate of low temperature modulus of 288 GPa falls in the range of high strain rate modulus determined by Prevorsek *et al.*,[26] confirming thus that, at low temperature and/or high strain-rates, the modulus of the ultra-strong PE fibers falls fairly close to the theoretical modulus of the crystalline domains. Considering the high degree of crystallinity of about 80%, high aspect ratio crystallites and crystalline orientation function close to unity, we would expect that the low temperature high deformation rate modulus of the ultra-strong PE fibers should fall above 250 GPa range, which is consistent with the presented experimental data.

STRENGTH

A great deal has been written about the theoretical strength of polyethylene fibers. The unresolved issues exist at several levels: the strength of an isolated molecule, the strength of an ensemble of perfectly oriented molecules, and the analysis of the achieved strength based on the morphological analysis.

Considerable differences already exist with regard to the strength of a single molecule. Based on the work of Crist,[27] we list in Table VII theoretical strength, modulus, elongation at break, and the activation energies for bond breakage of ethylene repeat units. Using these data, Prevorsek[28] calculates the theoretical strength of a perfect ensemble of extended polyethylene molecules as a function of the molecular weight. The calculations assume a random distribution of chain ends and a fracture mechanism consistent with Griffith's crack stability criteria.[29] The results are shown in Figure 21. Two features of these graphs must be noted. Large

TABLE VII

Theoretical strength σ^*, modulus E, elongation at break ϵ_B and activation energy ΔF^* of the ethylene repeat unit

σ^* (GPa)	E (GPa)	ϵ_B (%)	ΔF^* (J/bond)
66.00	405	43	3.39×10^{-19}
34.60	405	20	1.015×10^{-19}
19.25	59	33	0.467×10^{-19}
106.00	297	33	2.566×10^{-19}

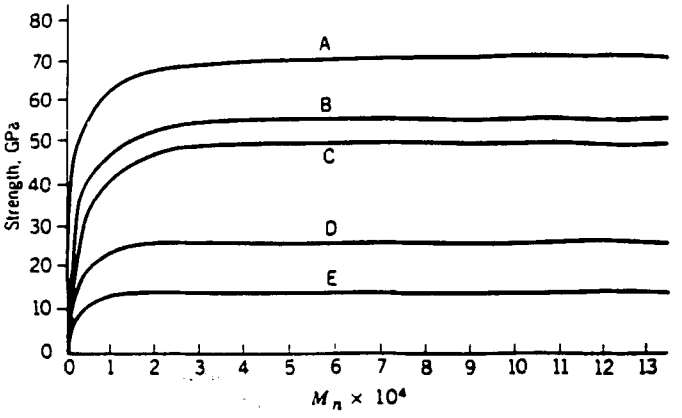

FIGURE 21 Dependence of strength of polyethylene fiber on molecular weight. Modulus and activation energies taken from studies of various authors. A: Crist *et al.*; B: Boudreaux (revised); C: Zhurkof *et al.*; D: Morse; E: Boudreaux.

variations in the theoretical strength at infinite molecular weight and the levelling of the strength at much lower molecular weights than is experimentally observed. It should also be noted that there is less agreement with regard to strength between various authors than with regard to modulus. Several authors consider values of the theoretical strength of 20 GPa acceptable.[30] The present authors on the other hand consider values of ~50 GPa more realistic. It should also be noted that the theory of Prevorsek[28,29] neglects the stress relaxation effects and is hence suitable only for the discussion of low temperature and high deformation rate strength.

With regard to the achieved strength, it should be noted that the commercially available products have strength between 3–4 GPa at ambient temperature and standard rates of deformation.

Several relationships are of scientific and technological interest. For example, a linear relationship between modulus and strength has been frequently reported. To illustrate this relationship, we show the data of van der Werff and Pennings[31] (Figure 22). In addition to the linear relationship between modulus and strength, these data also show some of the highest room temperature values of strength (~7 GPa) and modulus (~240 GPa) at low deformation rate ~0.43 min^{-1} but for relatively short samples (32.5 mm) and single filaments.

The differences in strength and modulus reported in Figure 22 are usually obtained by maintaining the spinning conditions constant but changing the draw ratio. An example of the effect of draw ratio on strength is shown in Figure 23. The important findings are; 1) the low strength (0.8 GPa) and ductility of the sample having draw ratio of 15 and 2) that an increase of draw ratio from 15 to 70 increases the strength of the fiber by a factor of 5.

The effect of deformation rate on strength is more difficult to investigate than that on modulus. This is because, with increasing rate of deformation the breakage of fibers becomes more frequent and a great deal of data has to be discarded. The effect of strain rate expressed as cross-head speed is shown in Figure 24 for a fiber

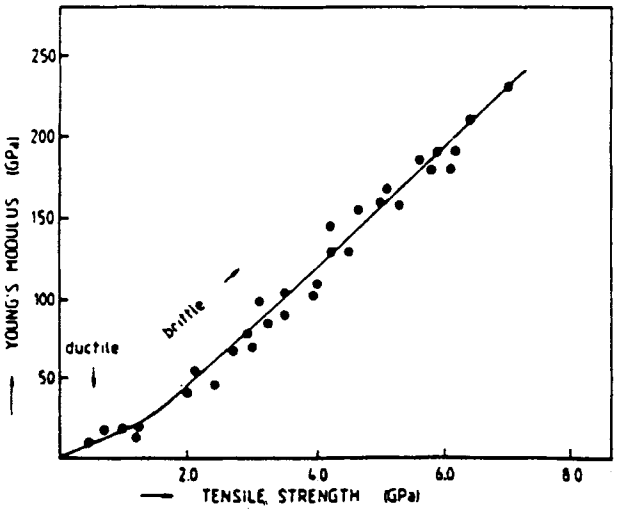

FIGURE 22 Young's modulus versus tensile strength of ultra-high molecular weight PE fiber.

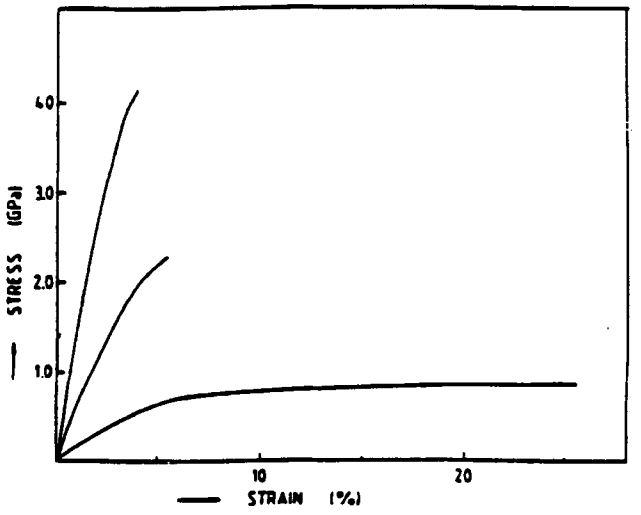

FIGURE 23 Effect of draw ratio on strength of ultra-high molecular weight PE fiber for a draw ratio of 15, 30 and 70.

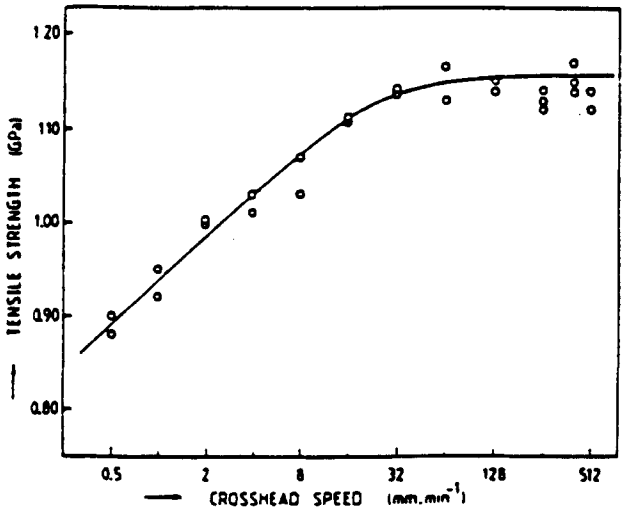

FIGURE 24 Effect of strain rate on tensile strength of ultra-high molecular weight PE fiber.

having a draw ratio of 15. The authors[31] propose that the levelling of the strength indicate a ductile brittle transition at ~32 nm/min cross-head speed beyond which the rate effects are much smaller.

Because of testing problems, we do not have at present reliable data on strength in technologically very important deformation rates encountered in explosions or impact of fast projectiles. In the absence of such data, we make use of temperature dependence of strength assuming that the time-temperature relationship as reflected in strain-rate temperature relationship and observed with modulus holds also for strength.

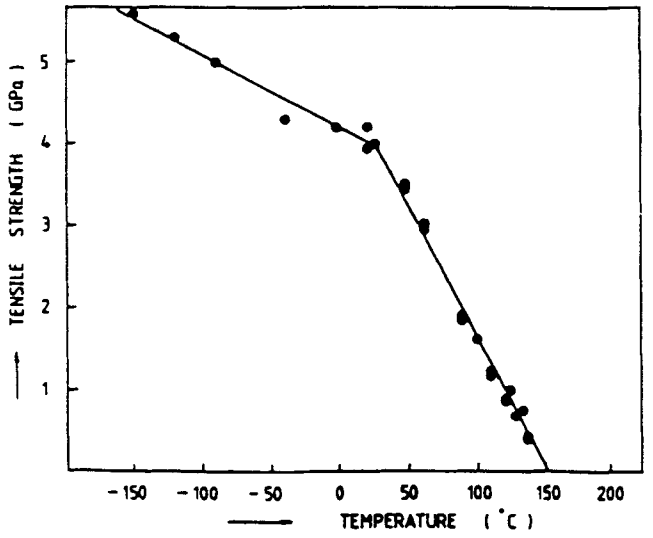

FIGURE 25 Effect of temperature on tensile strength of ultra-high molecular weight of PE fiber.

The tensile strength-temperature relationship for an ultra-high modulus PE fiber of draw ratio of ~100 is shown in Figure 25. This fiber has a strength of ~4 GPa at room temperature. On cooling the strength increases linearly with decreasing temperature and reaches 5.6 GPa at ~ −150°C. Based on this and similar results obtained by others, in our calculation involving ballistic impact (i.e., deformation rates exceeding 10^3 min^{-1}), we use a tensile strength that is about 40% higher than that measured at standard rates of deformation of ~1 min^{-1}. In the analyses of projectile armor interactions (deformation and penetration) on confinement of explosions, we therefore use a tensile strength of 5 GPa for Spectra 1000 fibers for deformation rates exceeding 10^3 min^{-1}.

ENERGY ABSORPTION POTENTIAL IN ARMOR

a. Straining in Tension

Considering the large strain rate effects discussed above and the fact that these effects are unique for PE, the relative merits of PE vs. other reinforcing fibers increase with the rate of deformation. Thus it is not surprising that Spectra is rapidly gaining acceptance in the technology of survival where the principal role of a component is to protect people, apparatus and equipment from blasts of explosions, fast moving projectiles etc. In the analysis and design of structures to absorb the energy of fast moving projectiles, we must therefore use the properties corresponding to the deformation rates caused by such impact. We pointed out that under such conditions Spectra modulus and stress fall in the range of ~280 GPa and ~5 GPa. This increases the energy absorption of Spectra products substantially above the values expected on the basis of testing experiments conducted at the rate of deformation used in standard testing procedures.

However, this factor alone is insufficient to establish the ranking of PE with respect to other materials. In ballistic mechanics, where the impact velocities approach the velocities of the strain propagation, it is also necessary to take into consideration the amount of material that experiences the stress during the duration of the impact. These times (duration of impact) are of the order of several microseconds and the amount of strained material is proportional to the velocity of strain propagation.

To determine the strain propagation rate in polyethylene, we used the transverse impact using two methods to treat the data. The results which depended a great deal on the data treatment, are summarized in Table VIII. In column A are shown the results obtained by treating the experimental data using the analytical procedure of Smith *et al.*[24] The column B, on the other hand, contains more recent data of Field *et al.*[32] based on the outputs of sensors placed at the points where the fibers are supported. The difference in PE/Kevlar strain propagation rate ratio 1.48 vs. 1.30 is somewhat larger than expected. The difference may be caused by much larger strain amplitude and pretension dependence of strain propagation rate in HDPE than in Kevlar. Work is in progress to resolve this problem.

Consider that at very fast rates of deformation, the energy absorption potential of a fiber broken in tension, W_{max}, equals

$$W_{max} = K \cdot W_f \cdot C \tag{1}$$

where K is a constant, W_f the energy to break of fibers at corresponding rates of deformation and C the strain propagation velocity. This expression enables us to estimate the relative energy absorption potential of HDPE and aramid fibers at ballistic rates of deformation. On the absence of the energy to break data we assume that both the fibers exhibit linear response up to their breaking point. Then,

TABLE VIII

Strain propagation rate of ultra-high strength polyethylene fiber

	A		B	
Fibers	Velocity (m/sec)	Modulus (GPa)	Velocity (m/sec)	Modulus (GPa)
PE	17,800	320	13,000	230
Kevlar	12,000	170	9,300	130
Elastomer	95-200			
PE/Kevlar Ratio	1.43		1.3	

Table VIII and the estimated high deformation rate strength of HDPE and Kevlar as 5 and 3 GPa respectively, we obtain the value of:

$$\frac{W_{max}(\text{HDPE})}{W_{max}(\text{Kevlar})} \approx 3.0 \pm 0.75$$

The relative penetration resistance falling in this range is indeed observed on the impact of large projectiles of ~1.5 cm in diameter, impact velocity of ≥2000 ft/sec and armor structures that are thicker than ~1.5 cm. These conditions of armor design and impact load insure that the predominant failure mode in the plate is straining of fibers in tension, a mode of failure that is predominant with larger size impactors and thicker plates.

A great deal of work, both experimental and analytical, has been dedicated to this issue of energy absorption. The studies in which the penetration resistance of Spectra and Kevlar composites were compared, frequently confirmed the expected energy absorption capacity ratio of four. There are, however, numerous cases where Spectra products are only marginally better or about equal to those of aramids. Those cases were relatively easy to explain, but to our surprise, there were also cases where the advantages of Spectra over other (aramid) products were much greater than expected on the basis of the energy absorption ratio of four.

To explain these data, it is necessary to review the principles of penetration dynamics as it is currently applied to fiber structures. A qualitative explanation of the cases where the impact energy absorption ratio of Spectra to equivalent Kevlar structures is less than one is quite simple. In the discussions of the relative energy absorption potential of Spectra vs. other fibers, our considerations were so far limited to straining in tension. In this mode of failure, Spectra has indeed a very large advantage over aramids. However, the failure frequently involves also the shear and compression and in these failure modes, the advantages of Spectra are much less. It must therefore be stated that the four-fold advantage of Spectra over Kevlar is expected only if the impact and composite design is such that the penetration involves primarily straining and breaking in tension.

b. Penetration Mechanisms

In the analysis of penetration of fiber reinforced composites, we currently consider three primary mechanisms: lateral displacement of fibers, breaking of fiber in shear, and straining and breaking of fiber in tension.

Schematically these failure modes are represented in Figure 26. A small pointed projectile can penetrate armor without breaking the fibers and in this case the penetration resistance depends on the composite construction: weave, yarn and fiber denier, matrix characteristics, and interfacial adhesion etc. The failure in shear and cutting is very important with sharp fragments. As the projectile diameter increases and with increasing thickness of the armor, the tension mode becomes more and more important. The penetration resistance of various composites in the above modes of failure can be studied using high speed testing equipment by firing projectiles of various geometries against targets. Systematic experimental and analytical work showed that in actual cases, all penetration modes exist and that their

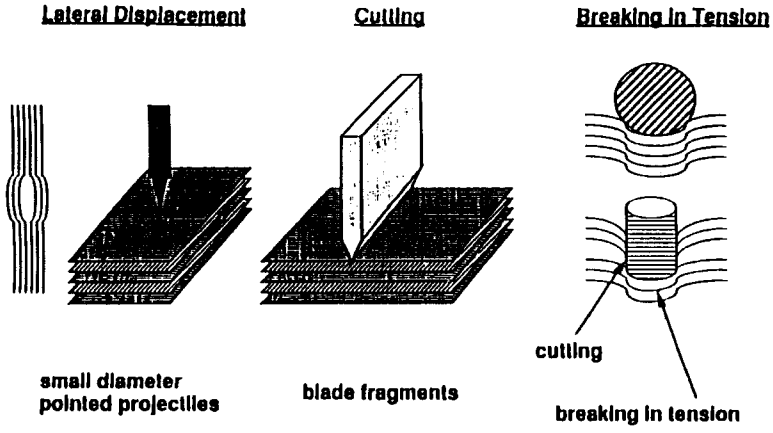

FIGURE 26 Three principal penetration failure modes of fiber reinforced armor.

relative importance can be greatly affected by their design. The penetration resistance corresponding to these modes of failure determined by instrumented impact testing and the relative levels of Spectra and aramids are shown in Figure 27.

In this respect it should be noted that relative values of shear strength or cut resistance were measured by both instrumented impact as well as firing of blade-like projectiles at high speed against suspended filaments. Both methods indicate a substantially higher cut resistance of Spectra compared to Kevlar. It should also be noted that our analyses of penetration of soft body armor and military helmets show that the penetration is primarily by cutting and lateral displacement of filaments because of specified projectile geometries and speeds. Hence, with soft body armor and helmets, the advantage of Spectra over aramids is due primarily to its superior cut resistance. With projectile larger than 1 cm in diameter and armor thicknesses exceeding 1.5 cm, the failure and straining in tension becomes a major factor.

c. Damage Tolerance

On the basis of these considerations, it is possible to explain and quantitatively analyze a great deal of experimental data. There are, however, observations and experiments that can be easily reproduced showing that, in some cases, the energy absorption potential of Spectra products exceeds the four-fold advantage over other composite by a wide margin. The following experiments illustrate these points.

Using Dynatap 8200 MST instrumented impacted tester, we evaluated a series of composites: The experiment yielded the following data:

- Load curve
- Maximum load value
- Energy absorption curve
- Energy absorbed at maximum load
- Total energy absorbed upon completion of impact

A typical data output for glass and Spectra composite of equivalent constriction

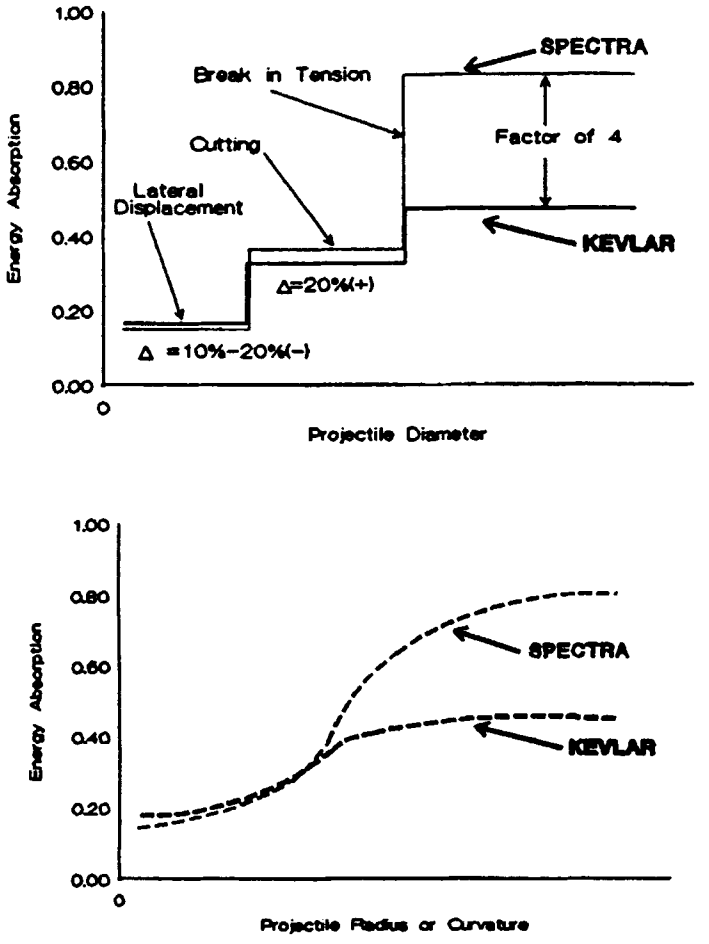

FIGURE 27 Qualitative representation of penetration resistance as energy absorption for the principal failure modes shown in Figure 26.

is shown in Figure 28. To compare various fibers, we constructed composites where the following construction parameters were held constant.

- Fabric plain weave construction
- Fabric weight 50–60 oz/yd^2
- Number of layers: 5
- Resin system: Araldit 6010 epoxy resin with HY956 hardener
- Fiber content by volume: 60%

The properties of fibers from which these composites were made are listed in Table IX.

The composite samples were tested under conditions indicated in Table X. The key observation is that S-2 glass, Kevlar and carbon fiber composites were penetrated at much lower impact energies. The load and energy data show that on the absorbed energy and peak loads were substantially higher than anticipated on the

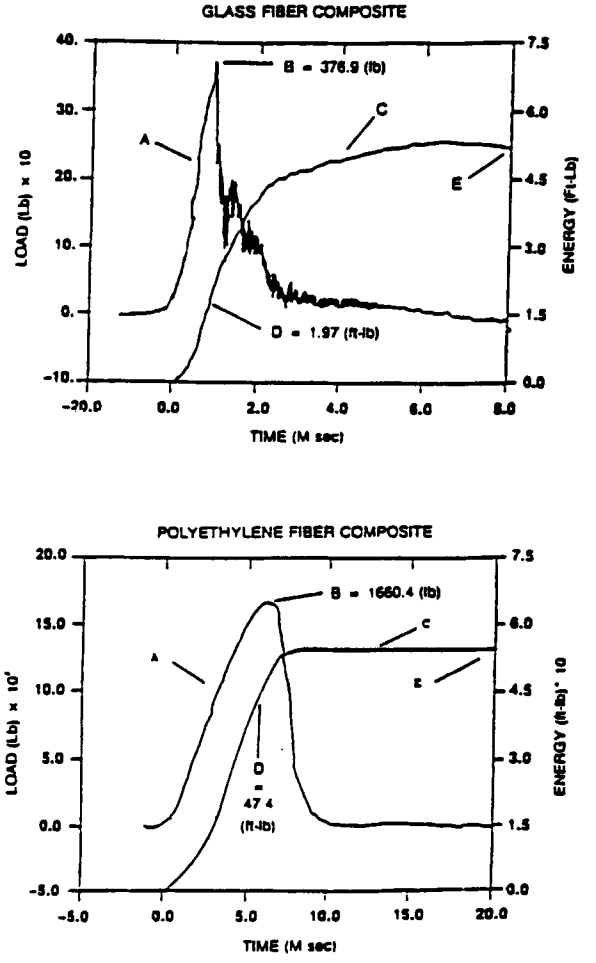

FIGURE 28 Instrumental impact: Load and energy outputs as function of time for—on weight basis—equivalent glass and Spectra fiber composites.

basis of the four-fold advantage discussed above. To some extent, this discrepancy could be attributed to the differences in sample preparation, namely, Spectra sample quality was superior to that of other samples. We consider this to be very unlikely but it must not be ruled out.

To broaden the data base and develop design criteria for penetration in damage tolerant structures, it was necessary to study the behavior of these composites on repeated impact. To accomplish this we subjected the Spectra 900 panel to the same impact conditions five times (namely 6.6 times the energy to penetrate the Kevlar 49 panel) and the Spectra panel survived all five impacts without failure (Table XI). Knowing that a 6.6 times impact energy to penetrate Kevlar panel must be very close to the energy required to penetrate the Spectra panel, we conclude that these panels can survive, without an apparent weakening, repeated impact at levels that are close to the energy required for their penetration.

To determine what happens in these composites on severe impact, we conducted

TABLE IX

Fiber properties

Property	UHSPE Spectra 900	Aramid HM	S-Glass	Graphite HM
Density, g/cc	0.97	1.44	2.49	1.86
Filament Diameter, micron	38	12	9	7
Elongation, %	3.5	2.5	5.4	0.6
Tensile strength, 10^3 psi	375	400	665	340
Specific strength, 10^6 in	10.7	7.7	7.4	5.0
Tensile modulus, 10^6 psi	17	19	13	50
Specific modulus, 10^6 in	495	365	140	750

HM = High Modulus

a series of experiments in which we progressively increased the impact energy from 6.6 to 9.6 times the energy to penetrate the Kevlar panel and recorded the force during the impacts. The peak force in four repetitive impacts is plotted in Figure 29, showing that the panel rigidity increased on repetitive impacts. This indicates that contrary to anticipated responses, namely a weakening of the test specimen and decrease of the panel modulus, the HDPE panels underwent on impact structural changes that enhanced their properties.

In the analysis of the behavior of composites under transverse impact, it must be recognized that the fibers on the impacted side experience compression and shear and that the tension is developed only on the back side of the panel. Consider further that, according to current estimates, the compression strength of polyethylene is significantly lower than that of aramids (by 30–60%) and, according to our data, the shear strength of PE is about 30% higher than that of aramids, and that the tensile strength at the rates of these experiments is possibly ~40% higher than that of aramids. It is obvious that this set of properties cannot explain large energy absorption differences between polyethylene and S-2 glass, aramid and carbon fiber composites. Based on the cited differences in compressive, shear and tensile strength, we could expect 50% increase in the penetration resistance, but an almost ten fold advantage recorded in these experiments shows that other energy absorption mechanisms must play a key role in the penetration resistance of these composites.

What is then the source of the energy absorption capacity that greatly exceeds the levels expected on the basis of strength data? Some of the answers are provided by inspection of targets after impacts that did not lead to penetration and after which the targets still retained almost the same energy absorption capability of the original sample. The microscopical examination of such samples shows, on the impact side, large plastic deformations of the fibers, flattening, and kink bands indicating shear as well as compressive failure. Since these shear and compressive

TABLE X

Instrumented impact single fiber systems

I.D.	No. of Layers	Fiber Ratio Spectra/Other	Laminate Construction	Maximum Load (Lb)		Energy (Ft-Lb) Maximum Load		Total		Ductility Index		Observations
				Actual	Index	Actual	Index	Actual	Index	Actual	Index	
Spectra 900	5	100/0	5S	1660.42	100	47.36	100	54.46	100	1.15	100	No penetration
S-2 Glass	5	0/100	5G	369.92	22	1.84	4	8.03	15	4.36	379	Penetration
Kevlar 49	5	0/100	5K	254.03	15	1.30	3	6.68	12	5.14	447	Penetration
HM Graphite	5	0/100	5Gr	133.10	8	1.28	3	2.52	5	1.97	171	Penetration

TABLE XI

Repetitive instrumented impact

Laminate	No. of Repetitive Impacts	Impact Energy (Ft-Lb)	Maximum Load (Lb)	Energy (Ft-Lb)				Observations
				Maximum Load		Total		
		Actual	Actual	Actual	%Abs*	Actual	%Abs*	
Spectra 900	1	57.0	2060	50.9	86	58.3	100	No Penetration
Spectra 900	2	57.0	3084	50.6	86	57.4	100	No Penetration
Spectra 900	3	59.0	3592	50.3	85	58.4	100	No Penetration
Spectra 900	4	59.0	3865	31.2	53	58.7	100	No Penetration
Spectra 900	5	80.0	4049	68.0	85	80.6	100	No Penetration
Spectra 900	6	95.4	4200	33.9	36	46.1	48	Penetration

* %Abs = per cent of the initial energy absorbed by the composite

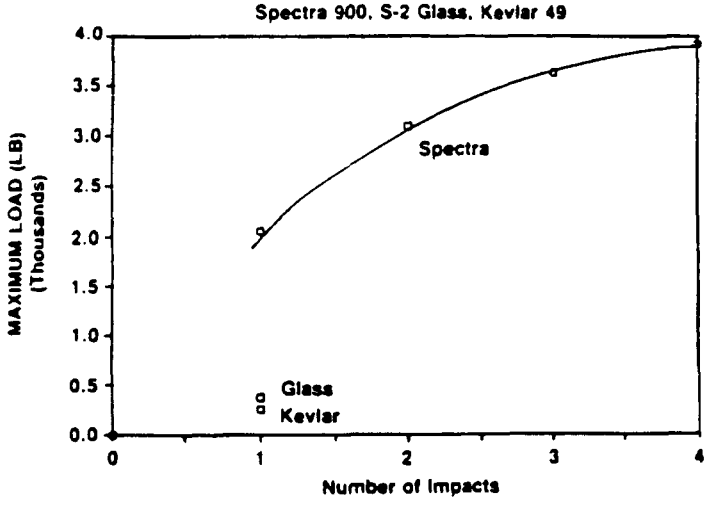

FIGURE 29 Change in the measured maximum load with repetitive impacts. Data for glass and Kevlar show the loads causing penetration. All tested composites had equivalent structures.

FIGURE 30 Electron microscopy of Spectra fiber indicating a well defined macrofibrillar (50 nm) and microfibrillar (5 nm) morphology. The macrofibrils and their dimensions are easily discerned at the upper right side of the micrograph.

failures of the fibers in the impact zone produced no readily detectable detrimental effects on the impact resistance of the panels, it means that polyethylene can, under certain conditions, fail in shear and compression and still retain their tensile properties essentially unchanged. Since it is the energy associated with the tensile mode of deformation into which the bulk of kinetic energy of the impacting body is transformed, these findings and observations explain at least qualitatively the observed behavior.

That also means that the key factor in the impact characteristic of PE composite discussed above is not the differences in the tensile strength, but the damage tolerance and capability of PE to undergo a variety of solid state deformation discussed in the previous sections without losing its ability to sustain large tensile loads and absorb energy in tension. Although the massive formation of kink bands is experimentally recorded in compressive failure, we can infer on the basis of these experiments that these compressive failures do not involve a great deal of breakage of primary bonds and that, upon subjecting the fibers that failed in compression to tension, the original tensile properties can, to a large degree, be restored.

d. Role of Microstructure in Damage Tolerance

The capability of polyethylene crystal to undergo solid state transformations without breakage of primary bonds is an important factor in the damage tolerance of Spectra fibers and composites. However, there are additional, and probably equally important contributions, that originate in the microstructure of these fibers. Electron microscopy of Spectra fibers (Figure 30) reveals a well defined and very regular microfibrillar (5 nm) and microfibrillar (50 nm) microstructure. A structural model showing the longitudinal view of the microfibril is presented in Figure 31. Based on the analyses of X-ray diffraction patterns from strained samples, we know that the amorphous domains connecting the crystals have a modulus of about 1–3 GPa, while the crystal modulus is close to its theoretical value of about 275 GPa.

The composite structure in which very strong crystals are covalently bonded to the surrounding rubbery matrix has an important role in the damage tolerance and impact resistance of Spectra® fibers.

The incorporation of a dispersed rubbery phase in brittle thermoplastics and thermosets is an approach widely used to improve the impact resistance of these systems. But the regularity of the Spectra rubbery and crystal phase structure has the characteristics of a macrolattice that gives rise to the SAXD patterns from which the presence of periodicity on the 5 and 100 nm scales is indicated.[33] This regularity of the macro-lattice has a strong positive effect on strength and energy to break because it reduces the fluctuations of the stress concentrations that would exist if the two phase structure was random.

Surprisingly, this nanometer composite structure has its counterpart in nature, namely in sea shells. Nacre, which constitutes the strong and impact-resistant component of the sea shell, is made of weak aragonite crystals bound by an organic elastomeric matrix containing chitin (Figure 32). This example illustrates, according to Sarikaya *et al.*,[34,35] an important design principle that evolved in nature to equip some slow moving and defenseless species with the damage tolerant armor essential for their survival.

AlliedSignal

Nano-Composite Structure of Spectra Fibers

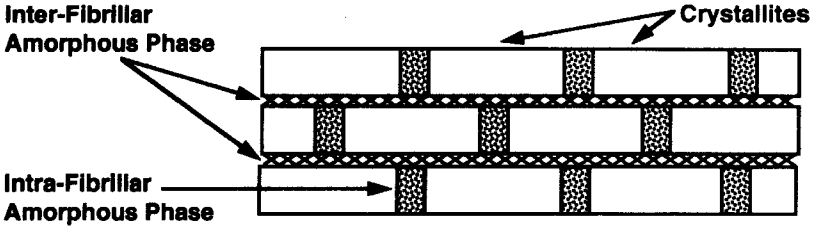

Modulus	Strength
PE(Crystal) = 280 GPa (~Diamond)	PE(Crystal) = 20-30 GPa
PE(Amorphous) = 2 GPa (Rubbery)	Aragonite = 0.2 GPa

FIGURE 31 Nano-composite structure of Spectra fibers.

AlliedSignal

Nano-Composite Structure of Sea Shells (NACRE)

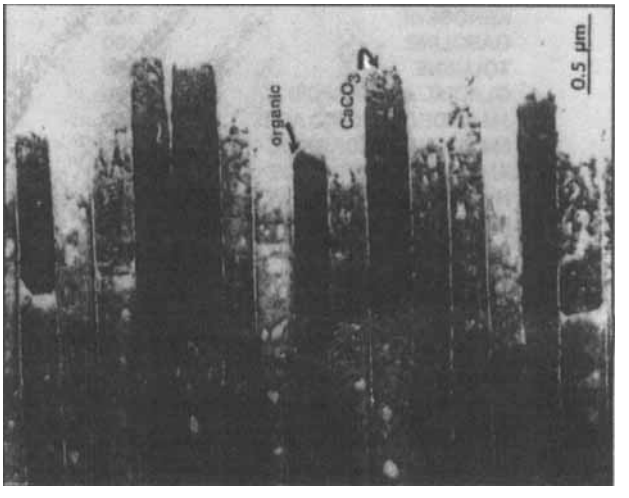

FIGURE 32 Nano-composite structure of Nacre in sea shells.

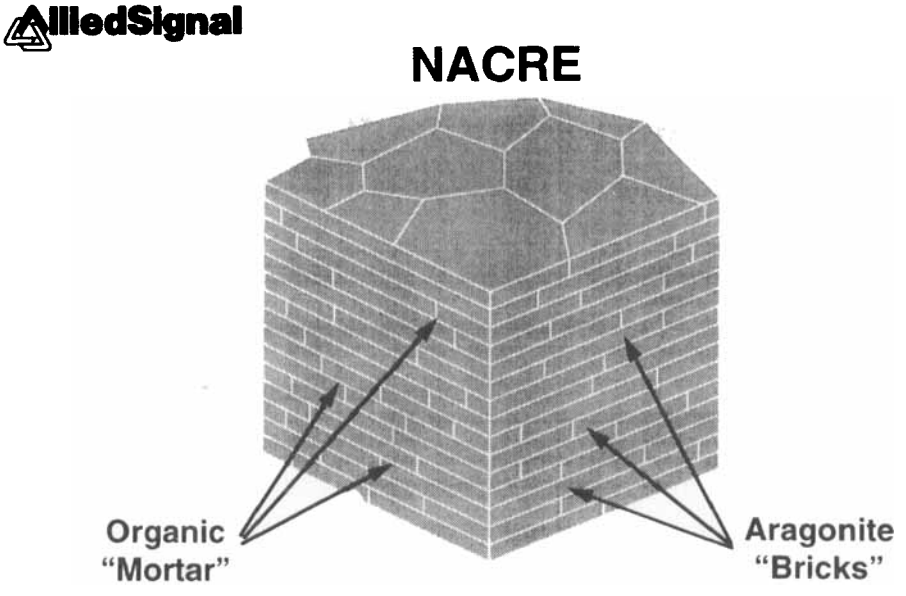

FIGURE 33 Model of mortar and brick structure of Nacre.

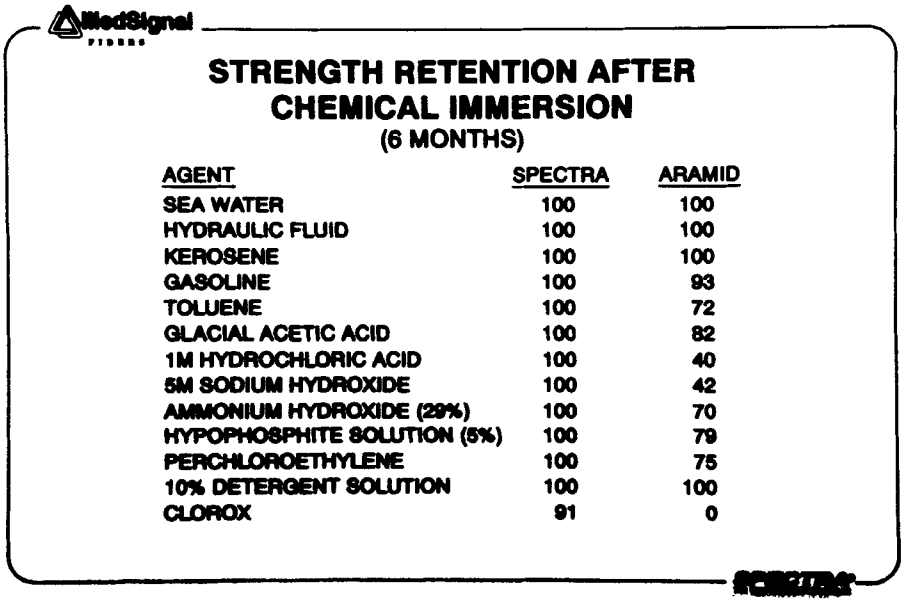

FIGURE 34 Strength retention after chemical immersion for Spectra and Aramid fiber.

In Spectra fibers, this Nacre "brick and mortar" composite structure (Figure 33) is relocated on approximately the same scale in one direction. However, in Spectra, the weak aragonite crystals are replaced with needle-like, nearly perfect crystals exhibiting (in one direction) a modulus approaching that of diamond and a strength of about 50 GPa. Since these crystals are covalently bonded to a rubbery matrix

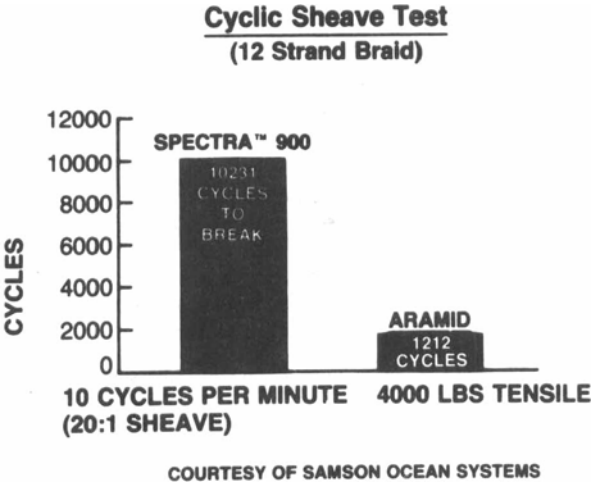

FIGURE 35 Data of cyclic sheave test for equivalent Spectra and aramid braids.

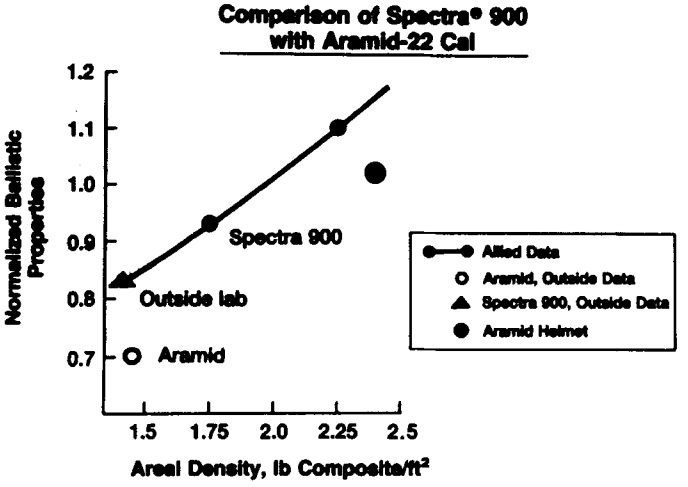

FIGURE 36 Normalized penetration resistance of Spectra and Aramid armor vs. 22 caliber fragment.

of the same molecules, the adhesion between the two phases is at optimum. In summary, the structure of Spectra fibers is not only the most damage tolerant and impact resistant synthetic structure made to date, but also the most energy absorbing structure we can currently conceive. And, as Nacre is used in the armor of sea mollusks, Spectra composites are used as armor for aircraft, vehicles and military and law enforcement personnel.

APPLICATIONS AND PRINCIPAL PERFORMANCE CHARACTERISTICS

The basic mechanical properties, namely the specific modulus and strength shown in Figure 1, qualify Spectra® for numerous applications. In comparison with the

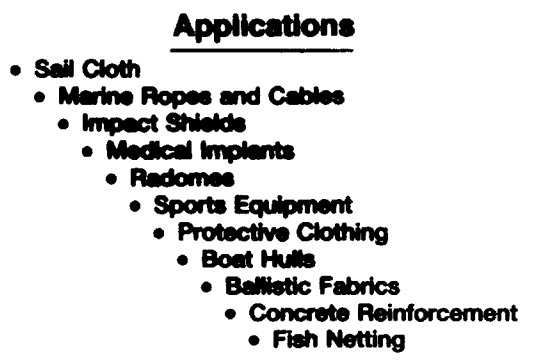

FIGURE 37 Typical applications for Spectra fibers and composites.

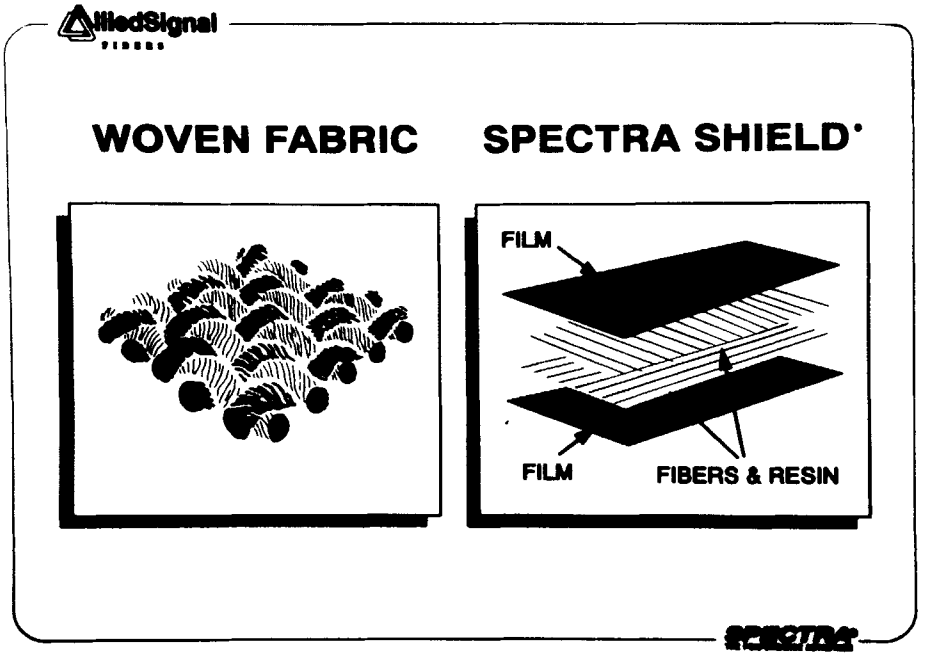

FIGURE 38 Schematic representation of woven fabric and Spectra Shield composite used in soft and rigid armor.

principal high performance organic fibers of aramid type, Spectra® fibers also excel in solvent and water resistance (Figure 34), flexural fatigue (Figure 35) and resistance to penetration of projectiles (Figure 36). With regard to the penetration resistance to projectiles, it must be noted that the relative performance advantage of Spectra® vs. aramid armor increases with the projectile diameter and projectile impact velocity. The theoretical (i.e. 3.5 fold) advantage has been observed with projectiles having diameters equal to or exceeding 1.5 cm.

It must be, however, recognized that these performance advantages decrease with increasing temperature. The following ceiling temperatures can be used as the guidelines: 100°C for stresses exceeding 1 GPa, 125–130°C for manufacturing,

and 135°C for confinement of explosions, armor and other application involving deformation rates equal to or exceeding $1 \times 10^2\ s^{-1}$.

Based on these performance characteristics, Spectra fibers are rapidly expanding their market share in a large number of applications. The more important ones are listed in Figure 37. In most armor applications, Spectra® is used in the form of Spectra Shield® type uniaxial composite shown in Figure 38. Spectra Shield® is commercially available as both a soft and rigid armor component. The soft type is used in personal armor while the rigid type is used in military helmets, aircraft luggage containers, armored vehicles, aircraft armor, etc.

CONCLUSIONS

The rapid acceptance of Spectra® must to a large degree be attributed to the unmatched damage tolerance, impact and fatigue resistance of this fiber. This fiber gets stronger, stiffer and tougher with increasing rate of deformation. This is contrary to other strong polymeric materials, which usually embrittle at high rates of deformations.

The primary cause of the exceptional damage tolerance and energy absorption of Spectra® originates, however, in the capability of polyethylene crystals to undergo solid state transformations without the breakage of primary bonds and their nanoscale composite structure. The microfibrils of Spectra® consist of long needle-like crystals, of nearly theoretical strength and modulus, that are covalently bonded to a rubbery matrix consisting of same molecules. This microstructure is analogous to that of Nacre in sea shells in which weak aragonite crystals are bonded by an elastomeric matrix containing chitin. In Spectra®, however, the weak aragonite crystals are replaced with ultra strong PE crystals capable of undergoing large solid state deformations and energy absorption. Therefore, we currently cannot conceive a more energy absorbing material.

References

1. A. J. Pennings and K. E. Menninger, in "Ultra High Modulus Polymers," A. Cifferi and I. M. Ward, eds., Applied Science Publishers, London, p. 117, 1979.
2. P. Smith, P. J. Lemstra, B. Kalb and A. J. Pennings, *Polymer Bulletin 1*, 733 (1979).
3. P. Smith and P. J. Lemstra, U.S. Patents Nos. 4,344,908, 4,422,993, 4,430,383.
4. S. Kavesh and D. C. Prevorsek, U.S. Patents Nos. 4,413,100, 4,536,536, 4,663,101.
5. D. C. Prevorsek, H. B. Chin and D. S. Cordova, Allied Signal Inc. Report.
6. D. T. Grubb, *Macromolecules*, article in press.
7. V. Kramer, Allied-Signal Inc., unpublished data.
8. A. Schaper, D. Zenke, E. Schultz, A. Hirte and M. Taege, *Phys. Stat. Sol. (a)*, **116**, 179 (1989).
9. D. H. Reneker and J. Mazur, *Polymer*, **24**, 1387 (1983); ibid, **29**, 3 (1988).
10. H. D. Keith and E. Passaglia, *J. Res. Natl. Bur. Std.*, **68A**, 513 (1964).
11. P. Predecki and W. O. Statton, *J. Appl. Phys.*, **37**, 4053 (1966).
12. M. Takayanagi, K. Imada and T. Kajiyama, *J. Polymer Sci., C*, **15**, 263 (1966).
13. I. Sakurada, I. Ito and K. Nakamae, *Macromol. Chem.*, **75**, 1 (1964); *J. Polymer Sci.*, **C15**, 75 (1966).
14. R. N. Britton, R. Jakeway and I. M. Ward, *J. Mater. Sci.*, **11**, 2057 (1976).
15. J. Clements, P. Jakeway and I. M. Ward, *Polymer*, **19**, 639 (1978).
16. K. Nakamae, T. Nishino and H. Ohkubo, *J. Macromol. Sci. Phys., B*, **30**, 1 (1991).

17. B. J. Kip, M. C. P. van Eijk and R. J. Meir, *J. Polym. Sci., Pert B Polym. Physics*, **29**, 99 (1991).
18. R. Young, unpublished data.
19. B. J. Kip, R. Tabaksblat, W. A. C. Roovers, R. J. Meier and F. A. H. M. Moonen in "Crystal and Molecular Deformation in Strained High Performance PE Fibers," DSM Research Report.
20. S. Murthy, Allied-Signal Inc., unpublished data.
21. L. R. G. Treloar, *Polymer*, **1**, 95 (1960).
22. M. J. S. Dewar, Y. Yamaguchi and S. H. Suck, *Chem. Phys.*, **43**, 145 (1979).
23. D. S. Boudreaux, *J. Polym. Sci., Polym. Phys.*, **11**, 1285 (1973).
24. J. C. Smith, F. L. McCrackin and H. F. Schiefer, *Textile Res. J.*, **28**, 288 (1958); ibid., **30**, 752 (1960).
25. P. J. Barham and A. Keller, *J. Polym. Sci., Polym. Lett.*, **17**, 591 (1979).
26. D. C. Prevorsek, H. B. Chin, Y. D. Kwon and J. E. Field, *J. Appl. Polymer Sci.: Appl. Polymer Symposium*, **47**, 45 (1991).
27. B. Crist, M. A. Ratner, A. L. Browder and J. R. Sabin, *J. Appl. Phys.*, **50**, 6047 (1979).
28. D. C. Prevorsek, Ultimate Properties, Uniaxial Systems, in "Encyclopedia of Polymer Science and Engineering," Supplemental Volume p. 803, Second Edition, John Wiley & Sons, Inc.
29. D. C. Prevorsek in "Polymers for Advanced Technologies," M. Levine, Ed., VCH Publishers, p. 557, 1988.
30. Y. Termonia, P. Meakin and P. Smith, *Macromolecules*, **18**, 2246 (1985).
31. H. van der Werff, Ph.D. Thesis, University of Groningen (Prof. Pennings promotor) April 26, 1991, pp. 31–58.
32. J. E. Field and Q. Sun, "High Speed Photography of Transversely Impacted Fibers: A Comparison of Spectra and Kevlar," Report prepared for Allied-Signal, June, 1990.
33. A. Schaper, D. Zenke, E. Schultz, R. Hirte and M. Taege, *Phys. Stat. Solid., (a)*, **116**, 179 (1989).
34. M. Sarikaya, K. E. Gunnison, Y. Yastreby and I. A. Aksay in "Materials Synthesis Utilizing Biological Processes," P. D. Calvert and M. Aplwe eds., p. 109 (MRS Symposium Series, Vol. 174) Materials Research Society.
35. D. C. Prevorsek, H. B. Chin and S. Murthy, *J. Polym. Sci: Polym. Symp.*, **75**, 81 (1991).